Synthesis, Structures, and Redox Properties of Mixed-Sandwich Complexes of Cyclopentadienyl and Hydrotris(pyrazolyl)borate Ligands with First-Row Transition Metals

Tim J. Brunker, Andrew R. Cowley, and Dermot O'Hare*

Inorganic Chemistry Laboratory, University of Oxford, South Parks Road, Oxford OX1 3QR, U.K.

Received January 7, 2002

A series of $[MCp^RTp]^{n+}$ (Cp^R = Cp*(pentamethylcyclopentadienyl) or Cp (cyclopentadienyl), Tp = hydrotris(pyrazolyl)borate) complexes have been synthesized by reaction of a suitable MCp^R precursor with KTp (Cp^R = Cp*; n = 0, M = Cr, Fe, Co, Ni; n = 1, M = Cr, Co, Ni; Cp^R = Cp; n = 0, M = V, Co, Ni; n = 1, M = V, Co). Oxidation with $[FeCp_2]^+$ salts or reduction with $CoCp_2$ where appropriate provided easy access to the corresponding M(III) or M(II) species. All of the complexes studied showed reversible M(III)/M(II) redox couples. Similarly $[MCp^RTpm]^{n+}$ complexes have also been isolated (Tpm = hydrotris(pyrazolyl)methane; Cp^R = Cp*, n = 1, M = Fe; Cp^R = Cp, n = 1 or 2, M = Co). Analytical, NMR, IR, and mass spectroscopic data are consistent with the formulation of these species as mixed-sandwich complexes. Oxidation of VCpTp in MeCN solution yields $[VCpTp(MeCN)]^+$, whereas similar reaction in CH_2Cl_2 solution yields $[VCpTp]^+$. $[VCpTp]^+$ reacts with σ-donor ligands L, where L = CN^tBu and PMe_3, to form $[VCpTpL]^+$ species, but is unreactive when L = CO, indicating little π-base character to the V center. Crystal structure determinations were performed for various complexes: CoCp*Tp is unique in displaying κ^2-Tp and η^5-Cp* coordination, whereas $[VCpTp]^+$, $[CoCp^*Tp]^+$, NiCp*Tp, and $[CoCpTpm]^{2+}$ all display mixed-sandwich structures with κ^3-Tp binding. The factors determining the relative conformations of the Cp^R and Tp ligands are discussed. The structures of $[VCpTp(MeCN)]^+$ and $[VCpTp(PMe_3)]^+$ were also determined and show that considerable distortion of the sandwich moiety has occurred to accommodate coordination of the extra ligand. For the MCp^RTp complexes a dependence of ν_{B-H} on Tp hapticity, ancillary ligand, and oxidation state is observed from IR spectroscopic data in the solid state. IR data obtained in solution suggest that CoCp*Tp is in conformational equilibrium, with a κ^3-Tp structure also present. Some of the factors affecting ^1H and ^{13}C NMR shifts are discussed and compared with relevant homoleptic analogues. Electrochemical data reveal, in general, that MCp_2 and MCp^*_2 species are more electron rich, although comparisons are best confined to a per metal basis.

Introduction

Hydrotris(pyrazolyl)borate (Tp) ligands have often been described as analogues to cyclopentadienyl (Cp) ligands, in that they are both monoanionic, six-electron donors which facially coordinate to a metal.[1] Thus Cp is often replaced by Tp in organo-transition metal systems as a way of modifying the reactivity of the metal center by changing its coordination environment and electronic properties.[2] Tp is the more sterically demanding ligand;[3,4] however, the relative electron-donating abilities of Tp, Cp, and their methylated analogues (Tp* = hydrotris(3,5-dimethylpyrazolyl)borate, and Cp* = pentamethylcyclopentadienyl) have been a matter of some debate. Pertinent data have been recently summarized and the conclusion has been drawn that no consistent trend was observable across the transition series and that donor ability is a function of the metal, its oxidation state, and the ancillary ligands.[5] As each ligand forms a series of simple sandwich complexes with most divalent first-row transition metals, ML_2 (MCp_2 is known for M = V−Ni, MCp^*_2 is known for M = Ti−Ni,[6] and MTp_2 is known for M = Ti−Zn[7]), we found it

(1) Trofimenko, S. *Chem. Rev.* **1993**, *93*, 943−980.
(2) For some recent leading references see (a) Ruba, E.; Simanko, W.; Mereiter, K.; Schmid, R.; Kirchner, K. *Inorg. Chem.* **2000**, *39*, 382−384. (b) Tellers, D. M.; Bergman, R. G. *Organometallics* **2001**, *20*, 4819−4832. (c) Sanford, M. S.; Henling, L. M.; Grubbs, R. H. *Organometallics* **1998**, *17*, 5384−5389. (d) Gutierrez-Puebla, E.; Monge, A.; Paneque, M.; Poveda, M. L.; Taboada, S.; Trujillo, M.; Carmona, E. *J. Am. Chem. Soc.* **1999**, *121*, 346−354.
(3) Maitlis, P. M. *Chem. Soc. Rev.* **1981**, 1−48.
(4) Rheingold, A. L.; Ostrander, R.; Haggerty, B. S.; Trofimenko, S. *Inorg. Chem.* **1994**, *33*, 3666−3676.
(5) Tellers, D. M.; Skoog, S. J.; Bergman, R. G.; Gunnoe, T. B.; Harman, W. D. *Organometallics* **2000**, *19*, 2428−2432.
(6) Elschenbroich, C.; Salzer, A. *Organometallics*; 2nd revised ed.; VCH: Weinheim, 1992.
(7) M = Ti: Kayal, A.; Kuncheria, J.; Lee, S. C. *Chem. Commun.* **2001**, 2482−2483. M = V and Cr: Dapporto, P.; Mani, F.; Mealli, C. *Inorg. Chem.* **1978**, *17*, 1323−1329. M = Fe − Zn: Trofimenko, S. *J. Am. Chem. Soc.* **1967**, *89*, 3170−3177.

10.1021/om0200149 CCC: $22.00
Publication on Web 06/18/2002

somewhat surprising that relatively few mixed-sandwich MCp^RTp species are known (Cp^R = Cp or Cp*). The synthesis and study of such complexes should provide further insight into the effects of replacing Cp^R with Tp at a transition metal center by direct comparison with the homoleptic sandwich analogues.

Previous studies of MCp^RTp complexes have been mainly confined to the case where M = Ru. RuCpTp was first synthesized by reaction of KTp with RuCp(COD)Cl (COD = 1,5-cyclooctadiene).[8,9] Similarly, reaction of $[RuCp^R(CH_3CN)_3]^+$ with a variety of poly(pyrazolyl)borate ligands gave a series of Ru(II) complexes (RuCpTp, RuCp*Tp, RuCp[B(pz)$_4$], and RuCpTp*), and the oxidized derivative $[RuCpTp^*]^+$ was also isolated.[10] A preliminary communication has reported the synthesis of $[Cp^RCoTp']^+$ from $CoCp^R(CO)I_2$ (Cp^R = Cp, Cp*; Tp′ = Tp, B(pz)$_4$) and $[RhCp^*Tp']^+$ from $[RhCp^*Cl_2]_2$ (Tp′ = Tp and B(pz)$_4$). This did not include any experimental details or characterizing data, however.[11] The authors did note their failure to prepare FeCpTp and NiCpTp from $FeCp(CO)_2Cl$ and $NiCp(PPh_3)Cl$, respectively. Several other references to attempted preparations of FeCpTp have also appeared; in each case the isolated products were $FeCp_2$ and $FeTp_2$.[10,12] The crystal structure of $[RhCp^*Tp]^+[PF_6]^-$ and preparative details for this and its B(pz)$_4$ analogue were subsequently reported in a full paper.[13] Some mixed Cp^R/Tp complexes of Ti and V were synthesized by Manzer,[14] including VCpTp, $TiCpTpCl_2$, TiCpTpCl, and $TiCp_2Tp'$ (Tp′ = Tp, B(pz)$_4$, and $H_2B(pz)_2$). Another related complex containing Cp, Tp, and ancillary CO ligands is the fluxional species Mo(κ^2-Tp)(η^5-Cp)$(CO)_2$.[15]

There has been some interest in preparing sandwich complexes with other carbocyclic aromatic ligands and Tp. The preparation of $[Ru(C_6H_6)Tp']^+$ (Tp′ = Tp and B(pz)$_4$) and the cyclobutadienyl complexes $[Co(Ph_4C_4)Tp]^+$ was also the subject of previous reports,[11] and the crystal structure of $[Ru(\eta^6\text{-}C_6H_6)(B(pz)_4]^+$ was subsequently described.[13,16] Several other Tp-containing species with a variety of substituted arenes have been isolated more recently, including $[Ru(C_6H_6)Tp^*]^+$,[17,18] and the reactivity of $[Ru(C_6H_6)Tp]^+$ (and other substituted-arene analogues) with nucleophiles has also been studied.[19,20] Mixed cyclooctatetraene (COT)/Tp′ (Tp′ = Tp and Tp*) sandwich complexes of Ti(III) have been reported, and the X-ray crystal structure of the Tp complex has been determined: the Ti center displays η^8-COT and κ^3-Tp bonding.[21] A series of trivalent lanthanide Tp′ sandwich complexes have also been prepared with COT as ancillary ligand, where Tp′ = Tp and Tp*.[22−24]

In this paper we report the systematic investigation of the synthesis of such complexes with 3d metals and their structural characterization and redox properties. We also report the synthesis of several mixed-sandwich complexes with hydrotris(pyrazolyl)methane (Tpm). Some of this work has appeared in preliminary form.[25,26]

Synthesis

In this work, we utilized the previously successful synthetic strategy of reacting Cp^RM half-sandwich complexes[27,28] containing labile ancillary ligands with the appropriate Tp anion. For Cp^R = Cp*, the availability of M(II) starting materials allowed ready access to the MCp*Tp species (where M = Cr (**1**), Fe (**2**), Co (**3**), and Ni (**4**)), as shown in Scheme 1. Only in the case where M = Fe did we find serious contamination of the product with species formed by ligand redistribution, $FeTp_2$ and $FeCp^*_2$. A mixture of $FeTp_2$ and **2** was isolated after recrystallization from pentane; the almost total insolubility of $FeTp_2$ in acetone allows the two components to be separated; however this is of limited use, as **2** is somewhat labile in solution, with subsequent crops of crystals containing $FeTp_2$ also. We hoped that a cationic species might be more stable; thus reaction of $[FeCp^*(MeCN)]^+$ with Tpm in MeCN solution gave $\mathbf{8}^+[PF_6]^-$, which could be isolated as a green solid by precipitation with Et_2O. $\mathbf{8}^+$ is also unstable in solution, with attempts to grow crystals leading to extensive decomposition. $[CoCp^*Cl]_2$ was found to be preferable to CoCp*(acac) as the starting material for the synthesis of **3**, as we found some contamination of the product with $CoTp_2$ in the latter case also. As yet, attempts to synthesize a MCp*Tp complex with Mn and V have been unsuccessful, maybe in part due to a lack of a suitable starting material. Reaction of $MnCl_2$ with 1 equiv each of LiCp* and KTp gave only the homoleptic species. Similarly, reaction of $[Cp^*VCl_2]_3$[29,30] with KTp or TlTp, or $VTpCl_2(THF)$[14] with Cp^*SnBu_3,[31] gave VTp_2 as the only isolable product. Formation of the mixed-sandwich complex by displacement of a Cp* ring from VCp^*_2[32] was also attempted: no reaction was observed to occur even after prolonged reflux and only starting material was recovered from the reaction mixture.

(8) Albers, A.; Oosthuizen, H. E.; Robinson, D. J.; Shaver, A.; Singleton, E. *J. Organomet. Chem.* **1985**, *282*, C49−52.
(9) Albers, M. O.; Robinson, D. J.; Shaver, A.; Singleton, E. *Organometallics* **1987**, *5*, 2199−2205.
(10) McNair, A. M.; Boyd, D. C.; Mann, K. R. *Organometallics* **1986**, *5*, 303−310.
(11) O'Sullivan, D. J.; Lalor, F. J. *J. Organomet. Chem.* **1973**, *57*, C58−60.
(12) Trofimenko, S. *Acc. Chem. Res.* **1971**, *4*, 17−22.
(13) Restivo, R. J.; Ferguson, G.; O'Sullivan, D. J.; Lalor, F. J. *Inorg. Chem.* **1975**, *14*, 3046−3052.
(14) Manzer, L. E. *J. Organomet. Chem.* **1975**, *102*, 167−174.
(15) Calderon, J. L.; Cotton, F. A.; Shaver, A. *J. Organomet. Chem.* **1972**, *38*, 105−111.
(16) Restivo, R. J.; Ferguson, G. *J. Chem. Soc., Chem. Commun.* **1973**, 847−848.
(17) Bhambri, S.; Tocher, D. A. *Polyhedron* **1996**, *15*, 2763−2770.
(18) Bhambri, S.; Tocher, D. A. *J. Chem. Soc., Dalton Trans.* **1997**, 3367−3372.
(19) Vol'kenau, N. A.; Bolesova, I. N.; Shul'pina, L. S.; Kitaigorodskii, A. N. *J. Organomet. Chem.* **1984**, *267*, 313−321.
(20) Bhambri, S.; Bishop, A.; Kaltsoyannis, N.; Tocher, D. A. *J. Chem. Soc., Dalton Trans.* **1998**, 3379−3390.
(21) Kilimann, U.; Noltemeyer, M.; Schafer, M.; Herbst-Irmer, R.; Schmidt, H.-G.; Edelmann, F. T. *J. Organomet. Chem.* **1994**, *469*, C27−C30.
(22) Kilimann, U.; Edelmann, F. T. *J. Organomet. Chem.* **1993**, *444*, C15−C17.
(23) Unrecht, B.; Jank, S.; Reddmann, H.; Amberger, H.-D.; Edelmann, F. T.; Edelstein, N. M. *J. Alloys Compd.* **1996**, *250*, 383−386.
(24) Amberger, H.-D.; Jank, S.; Reddmann, H. *Mol. Phys.* **1996**, *88*, 1439−1458.
(25) Brunker, T. J.; Barlow, S.; O'Hare, D. *Chem. Commun.* **2001**, 2052−2053.
(26) Brunker, T. J.; Green, J. C.; O'Hare, D. *Inorg. Chem.* **2002**, *41*, 1701−1703.
(27) Poli, R. *Chem. Rev.* **1991**, *91*, 509−551.
(28) Poli, R. *Chem. Rev.* **1996**, *96*, 2135−2204.
(29) Abernethy, C. D.; Bottomley, F.; Decken, A.; Thompson, R. C. *Organometallics* **1997**, *16*, 1865−1869.
(30) Aistars, A.; Newton, C.; Rubenstahl, T.; Doherty, N. M. *Organometallics* **1997**, *16*, 1994−1996.
(31) Herrmann, W. A.; Kalcher, W.; Biersack, H.; Bernal, I.; Creswick, M. *Chem. Ber.* **1981**, *114*, 3558−3571.
(32) Robbins, J. L.; Edelstein, N.; Spencer, D.; Smart, J. C. *J. Am. Chem. Soc.* **1982**, *104*, 1882−1893.

Scheme 1. Synthesis of MCp*Tp and MCp*Tpm Complexes

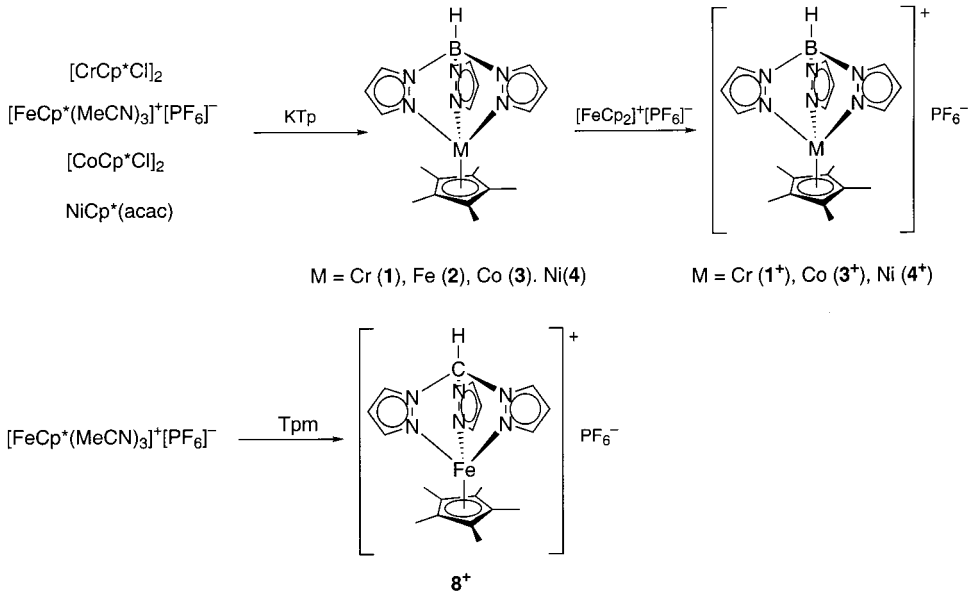

Scheme 2. Synthesis and Oxidation Chemistry of VCpTp

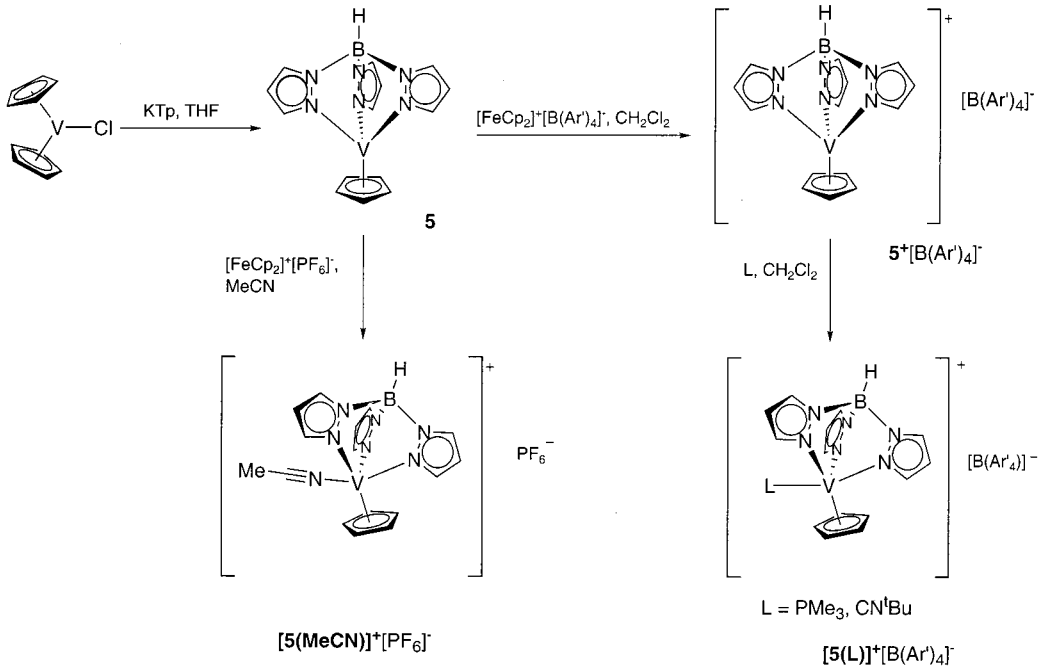

Oxidation of MCp*Tp to the corresponding M(III) species (where M = Cr, Co, and Ni) was achieved by reaction with $[FeCp_2]^+[PF_6]^-$. For M = Cr and Ni, the reaction was performed in THF solution, from which the $[PF_6]^-$ salts of $\mathbf{1}^+$ and $\mathbf{4}^+$ precipitated. The oxidation of **3** to $\mathbf{3}^+[PF_6]^-$ was carried out in MeCN; however use of this solvent in the oxidation of **4** did not lead to $\mathbf{4}^+[PF_6]^-$, but a light brown solid whose identity is unclear (vide infra).

We followed Manzer's route for the synthesis of VCpTp, **5**, by the reaction of VCp_2Cl with KTp in THF, as shown in Scheme 2. Adopting a slight modification to the workup procedure enabled isolation of clean **5** in 57% yield. This is an unusual reaction involving reduction of V(III) and displacement of a Cp^- ligand; however we were unable to identify the dark purple oily byproduct that was also formed. Degradation of Tp ligands in reaction with V(III) species has been observed in several instances, and such a process may be occurring here.[33] Reaction of VCp_2 with 1 equiv of KTp in THF was also found to produce **5**, although this approach is less satisfactory, as varying amounts of VTp_2 were also isolated. Cp displacement reactions are well known for VCp_2;[34,35] presumably Tp is a sufficiently strong ligand to displace both rings. The affinity of V(II) for N donor ligands has also previously been noted.[36]

Oxidation of **5** in MeCN with $[FeCp_2]^+[PF_6]^-$ gave a blue-green crystalline solid identified as $[VCpTp(MeCN)]^+[PF_6]^-$, $\mathbf{5}(MeCN)^+[PF_6]^-$, the 16-electron mono-

(33) Etienne, M. *Coord. Chem. Rev.* **1996**, *156*, 201−236.
(34) Jonas, K.; Wiskamp, V. *Z. Naturforsch. B* **1983**, *38b*, 1113−1121.
(35) Jonas, K. *Angew. Chem., Int. Ed. Engl.* **1985**, *24*, 295−311.
(36) Edema, J. J. H.; Stauthamer, W.; van Bolhuis, F.; Gambarotta, S.; Smeets, W. J. J.; Spek, A. L. *Inorg. Chem.* **1990**, *29*, 1302−1306.

Scheme 3. Synthesis of MCpTp and MCpTpm Complexes of Co and Ni

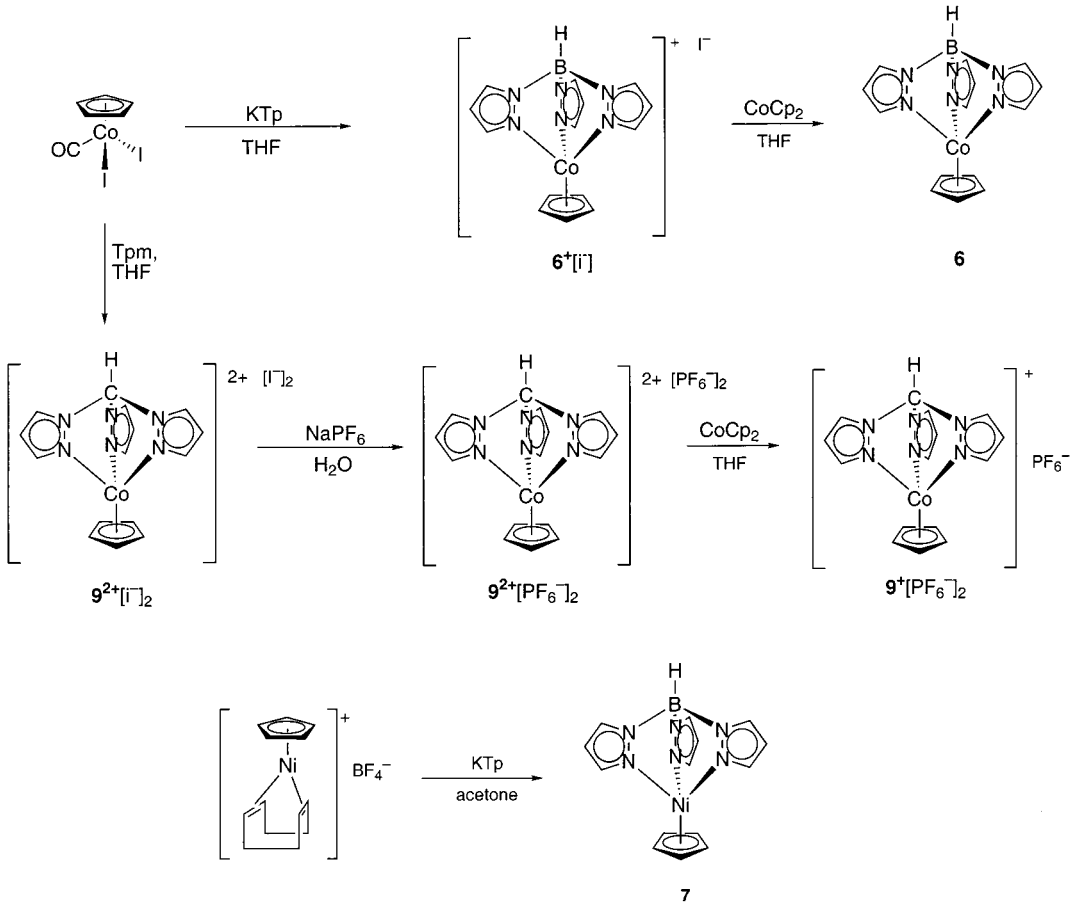

MeCN adduct of $\mathbf{5}^+$. Oxidation of **5** was performed in the absence of a coordinating solvent by reaction with $[FeCp_2]^+[BAr'_4]^-$ (Ar′ = 3,5-bis(trifluoromethyl)phenyl) in CH_2Cl_2. $[BAr'_4]^-$ is well known as a noncoordinating counterion,[37] and the solubility it confers on metallocenium salts has recently been demonstrated.[38] $[FeCp_2]^+[BAr'_4]^-$ is soluble in both Et_2O and CH_2Cl_2, allowing its use as a homogeneous oxidant in these solvents. A deep pink solid was isolated and identified as the unsolvated 14-electron V(III) species $[VCpTp]^+[BAr'_4]^-$, $\mathbf{5}^+[BAr'_4]^-$. Oxidation of VCpTp in acetone solution with $[FeCp_2]^+[PF_6]^-$ initially gave a green-blue solid, presumably $[VCpTp(acetone)]^+[PF_6]^-$, which on drying in vacuo slowly turned orange-brown. The IR spectrum of this solid closely resembled that of $\mathbf{5}^+$. Redissolution of this solid in acetone regenerated the blue-green solution. Similarly, addition of THF to solid $[VCpTp]^+[PF_6]^-$ turned the solid from red-brown to green: removal of the solvent in vacuo regenerated the red-brown solid. Addition of Et_2O to a solution of $\mathbf{5}^+[BAr'_4]^-$ in CD_2Cl_2 caused no color change, and the resonances of the cation remained unchanged in the ^1H NMR spectrum, indicating no adduct formation in this case.

In light of this behavior, further investigations into the coordinating properties of $\mathbf{5}^+$ were conducted. Thus oxidation of **5** with $[FeCp_2]^+[BAr'_4]^-$ in CH_2Cl_2 followed by treatment with excess CN^tBu or PMe_3 led to an immediate color change from dark red to blue-green and the isolation of a light blue solid after workup. Elemental analysis data were consistent with the formation of the adducts $[VCpTp(CNBu^t)]^+[BAr'_4]^-$, $\mathbf{5}(CNBu^t)^+[BAr'_4]^-$, and $[VCpTp(PMe_3)]^+[BAr'_4]^-$, $\mathbf{5}(PMe_3)^+[BAr'_4]^-$. Attempts to bind CO to $\mathbf{5}^+$ were unsuccessful however. Oxidation of **5** in acetone under a CO atmosphere yielded a brown solid after removal of solvent, whose IR spectrum contained no CO stretches and was similar to that of $\mathbf{5}^+$. Treatment of $\mathbf{5}^+[BAr'_4]^-$ in CH_2Cl_2 with CO under elevated pressure (5 bar CO pressure in a Fischer-Porter bottle) again yielded only starting material.

For the synthesis of mixed Cp/Tp Co complexes, we first synthesized the Co(III) species by the reaction of $CoCp(CO)I_2$ with KTp in THF (Scheme 3). A dark purple precipitate, $[CoCpTp]^+[I]^-$, $\mathbf{6}^+[I]^-$, was isolated in almost quantitative yield. The reduction of $\mathbf{6}^+[I]^-$ with $CoCp_2$ in THF then proceeds smoothly to give good yields of CoCpTp, **6**. The success of this route prompted us to attempt to synthesize $[CoCpTp^*]^+$ by the analogous reaction with KTp*. However, instead of the putative mixed-sandwich complex, we isolated CoTp*I.[39] In this reaction the starting material has been reduced from Co(III) to Co(II) in conjunction with displacement of Cp^-, CO, and I^-. No other Co-containing product was identified, so it is assumed that a corresponding organic-based oxidation is occurring. The Tpm analogue $[CoCpTpm]^{2+}[I]^-_2$, $\mathbf{9}^{2+}[I]^-_2$, was formed on reaction of $CoCp(CO)I_2$ with Tpm in THF. Reduction of $\mathbf{9}^{2+}$ (as its $[PF_6]^-$

(37) Brookhart, M.; Grant, B.; Volpe, A. F., Jr. *Organometallics* **1992**, *11*, 3920−3922.

(38) Chavez, I.; Alvarez-Carena, A.; Molins, E.; Roig, A.; Maniukiewicz, W.; Arancibia, A.; Arancibia, V.; Brand, H.; Manriquez, J. M. *J. Organomet. Chem.* **2000**, *601*, 126−132.

(39) Brunker, T. J.; O'Hare, D. Unpublished results.

salt) with $CoCp_2$ in THF lead to the formation of a yellow solid. Analysis and ^{1}H NMR spectroscopy of this material were consistent with a mixture of the desired product $[CoCpTpm]^+[PF_6]^-$, $\mathbf{9}^+[PF_6]^-$, and $[CoCp_2]^+[PF_6]^-$; however we were unable to further purify this mixture by fractional crystallization. Further attempts to reduce $\mathbf{9}^{2+}$ with the anionic complex $[MnCp^*_2]^-$ [40] (thus leaving a neutral byproduct) also resulted in the isolation of a similar mixture, leading us to conclude that $\mathbf{9}^+[PF_6]^-$ is labile in solution, forming $[CoCp_2]^+$ as a decomposition product.

For the synthesis of NiCpTp, **7**, we turned to $[NiCp(COD)]^+[BF_4]^-$ (COD = 1,5-cyclooctadiene) as a NiCp source;[41] the reaction of $NiCpCl(PPh_3)$ with KTp has been reported to not give the desired mixed-sandwich product.[11] Thus reaction with KTp in acetone solution gave, after recrystallization from pentane, **7** as well as quantities of $NiTp_2$ and $NiCp_2$. This reaction is capricious; repetition under the same conditions gave these products in varying ratios, and in some reactions no **7** was observed at all. **7** and $NiCp_2$ can be separated by sublimation of $NiCp_2$; nevertheless only small amounts of **7** could be isolated at any one time. We found that use of other solvents (MeCN, THF, and nitromethane) gave $NiTp_2$ as the only isolable species. ($[NiCp(COD)]^+[BF_4]^-$ is insoluble in THF, unstable in MeCN, but stable and soluble in nitromethane.)

Attempts to form MCpTp complexes (where M = Cr and Mn) by reaction of KTp with $CrCp_2$ and MnCpCl(TMEDA) (TMEDA = *N*,*N*,*N*′,*N*′-tetramethylethylenediamine) both resulted in the isolation of MTp_2 only. In contrast to the reaction with VCp_2, the second Cp displacement from $CrCp_2$ appears to be faster than the first.

Properties

The neutral M(II) Cp^R/Tp complexes are soluble in hydrocarbon, aromatic, ethereal, halogenated, and polar solvents (such as acetone and MeCN). **2** is most unstable in CH_2Cl_2 solution, with decomposition to unidentified products complete within several hours. As solids, **2**, **4**, and **7** are stable in air for short periods, but in solution all the M(II) species should be treated as air-sensitive. The neutral complexes do not sublime easily. The $[M(III)]^+[PF_6]^-$ salts are most soluble in MeCN or acetone and are generally air-stable as solids and in solution. $\mathbf{4}^+[PF_6]^-$ is unstable in solution, and its decomposition was followed by ^{1}H NMR spectroscopy of a solution in acetone-d_6, whereby the initial set of resonances attributed to the product are slowly replaced by a second set of paramagnetically shifted peaks.[42] The electrospray mass spectrum of $\mathbf{4}^+$ contained a low-intensity peak corresponding to the cation as well as various fragmentation peaks, of which the two of highest intensity correspond to the fragments $[NiTp + MeOH]^+$ and $[NiTp]^+$. (MeOH is utilized as the carrier solvent in the spectrometer.) The IR spectrum of the product of oxidation of **4** in MeCN solution contained absorptions at 2480 cm^{-1} (ν_{B-H}) and at 2318 and 2291 cm^{-1}, which can be attributed to coordinated MeCN. All these observations support the notion that $\mathbf{4}^+$ is labile in coordinating solvents and that $[TpNi(solvent)_x]$ adducts are readily formed. $[NiCp_2]^+$ is also of low stability in solution.[43]

The $[I]^-$ salts of $\mathbf{6}^+$ and $\mathbf{9}^{2+}$ were found to be much less soluble than those with $[PF_6]^-$ counterions; anion exchange could be readily performed by simple metathesis reactions. $\mathbf{9}^{2+}[I]^-_2$ is soluble only in H_2O but slowly decomposes in aqueous solution; however exchange of $[I]^-$ for $[PF_6]^-$ renders $\mathbf{9}^{2+}$ soluble and stable in polar organic solvents. A noticeable feature of the solid $[I]^-$ salts of $\mathbf{6}^+$ and $\mathbf{9}^{2+}$ is that they are considerably darker in color than their $[PF_6]^-$ analogues. This may be due to an I^- to cation/dication charge-transfer transition in the solid state. Similar behavior has been seen for $[CoCp_2]^+[I]^-$, which shows an $[I]^-$ to metal charge-transfer band in solution.[44] The electronic spectra of both species in solution were not counterion dependent and were superimposable, so this charge-transfer process is presumably confined to the solid.[45] The Tpm complexes are distinctly more soluble than their Tp analogues; for example $[FeCp^*Tpm]^+[PF_6]^-$ is much more soluble in CH_2Cl_2 than $[CoCp^*Tp]^+[PF_6]^-$.

Characterization

Table 1 summarizes the basic characterizing data for all compounds. The identity of the products was initially established by elemental analysis and mass spectroscopy. IR spectroscopy provides a convenient method of identifying the Tp complexes, particularly the paramagnetic species, with characteristic absorptions for ν_{B-H} and many strong absorptions in the fingerprint region. ^{1}H and ^{13}C NMR spectroscopy of the diamagnetic complexes (data are given in Tables 3 and 4) showed resonance patterns consistent with three equivalent pyrazolyl rings and unrestricted rotation of the Cp^R ring on the NMR time scale. The spectra of the $[PF_6]^-$ and $[I]^-$ salts of $\mathbf{6}^+$ and $\mathbf{9}^{2+}$ are essentially identical, suggesting that the I^- ligand is not participating in the coordination sphere of the metal in the latter case. At room temperature in solution, **2** displays a ^{1}H NMR spectrum typical of a paramagnetic species (see Table 5); however in the solid-state this complex is diamagnetic. The solution spectrum shows a marked temperature dependence which we have interpreted as arising from a spin equilibrium between $S = 0$ and $S = 2$ electronic configurations in solution. In contrast, $\mathbf{8}^+$ is diamagnetic in solution at room temperature, an observation that again illustrates the subtle dependence of spin states in Fe(II) complexes on structure.

SQUID magnetometry was used to determine the spin state of the paramagnetic complexes in the solid state, and the observed moments at 300 K are given in Table 1. We have previously noted the difference in spin states between **3** (low spin) and **6** (high spin)[25] and the high-spin state of **1**.[26] The other complexes display moments consistent with the expected ground states, although also worthy of note is the $S = 1$ ground state of the V(III) species, $\mathbf{5}^+$. A more detailed report on the magnetic

(40) Robbins, J. L.; Edelstein, N. M.; Cooper, S. R.; Smart, J. C. *J. Am. Chem. Soc.* **1979**, *101*, 3853−3857.
(41) Salzer, A.; Court, T. L.; Werner, H. *J. Organomet. Chem.* **1973**, *54*, 325−330.
(42) The resonances of the paramagnetic decomposition species are δ = 57, 43, and −10; integration 6:6:1 (and a set of resonances attributable to a diamagnetic species).
(43) Gribble, J. D.; Wherland, S. *Inorg. Chem.* **1990**, *29*, 1130−1132.
(44) Bockman, T. M.; Chang, H.-R.; Drickamer, H. G.; Kochi, J. K. *J. Phys. Chem.* **1990**, *94*, 8483−8493.
(45) Brunker, T. J.; Green, J. C.; Barlow, S.; O'Hare, D. Manuscript in preparation.

Table 1. Basic Characterizing Data for MCp^RTp and MCp^RTpm Complexes

compound	color	anal. found (calc) C	H	N	IR data (cm^{-1})[b]	MS[c] (*m*/*z*)	μ_{eff} (μ_B)[f]
CrCp*Tp,**1**	dark purple	57.07(57.02)	6.16(6.30)	21.01(21.00)	2457	400	5.02
$[CrCp^*Tp]^+[PF_6]^-$, $\mathbf{1}^+$	mauve	41.70(41.86)	4.70(4.62)	14.90(15.41)	2519, 839[PF_6]	400[d]	3.73
FeCp*Tp, **2**	blue-green	56.03(56.47)	6.17(6.24)	21.12(20.80)	2463	336[e]	*g*
CoCp*Tp, **3**	red-brown	55.85(56.04)	6.16(6.19)	20.06(20.64)	(2448), 2435, (2404)	407	1.85
$[CoCp^*Tp]^+[PF_6]^-$, $\mathbf{3}^+$	dark blue	41.38(41.33)	4.68(4.56)	15.25(15.22)	2505, 838[PF_6]	407[d]	
NiCp*Tp, **4**	golden brown	56.33(56.08)	6.18(6.19)	20.65(20.65)	2460	406	2.93
$[NiCp^*Tp]^+[PF_6]^-$, $\mathbf{4}^+$	black/brown	41.03(41.35)	4.69(4.57)	14.73(15.23)	2496	406[d]	1.91
VCpTp, **5**	mid-green	50.91(51.10)	4.59(4.59)	25.57(25.54)	2509	329	3.69
$[VCpTp]^+[BAr'_4]^-$, $\mathbf{5}^+$	deep pink	46.20(46.34)	2.57(2.28)	7.05(7.05)	2518		2.81
$[VCpTp(MeCN)]^+[PF_6]^-$, **5**$(MeCN)^+$	pale blue	37.49(37.31)	3.57(3.52)	19.06(19.04)	2497; 2312 [MeCN], 2286[MeCN]		2.78
$[VCpTp(CN^tBu)]^+[BAr'_4]^-$, **5**$(CN^tBu)^+$	pale blue-green	47.88(48.03)	3.21(2.84)	7.76 (7.69)	2501, 2212 [CN^tBu]		
$[VCpTp(PMe_3)]^+[BAr'_4]^-$, **5**$(PMe_3)^+$	pale blue-gray	46.45(46.40)	2.62(2.86)	6.72(6.63)	2538		
CoCpTp, **6**	yellow-green	49.83(49.89)	4.53(4.49)	24.79(24.93)	2494	337	5.80
$[CoCpTp]^+[I]^-$, $\mathbf{6}^+$	purple	36.22(36.24)	3.39(3.26)	18.09(18.11)	2501	337[d]	
NiCpTp, **7**	light green	50.30(49.92)	4.93(4.49)	25.00(24.95)	2472	337($M^+ + H$)	
$[FeCp^*Tpm]^+[PF_6]^-$, $\mathbf{8}^+$	green	42.41(43.66)	4.98(4.58)	15.71(15.27)	839[PF_6]		
$[CoCpTpm]^{2+}[PF_6]^-_2$, $\mathbf{9}^{2+}$	purple	28.96(28.68)	2.48(2.41)	13.89(13.38)	839[PF_6]	338, 169[d]	
$[CoCpTpm]^+[PF_6]^-$, $\mathbf{9}^+$	yellow	36.61(37.06)[a]	2.77(3.11)[a]	14.54(14.52)[a]	839[PF_6]		

[a] Complex was not isolated free of $[CoCp_2]^+$; calculated analysis is for composition $[CoCp_2PF_6]_1[CoCpTpmPF_6]_{3.5}$. [b] Spectra recorded as KBr disks, and unless otherwise indicated, data refer to ν_{B-H}. [c] All EI mass spectra unless otherwise indicated. [d] Spectra measured by ES in MeOH or MeCN. [e] $M^+ - pzH$. [f] As measured by SQUID magnetometry at 300 K. [g] This compound is diamagnetic as a solid at 300 K, but paramagnetic at room temperature in solution.

Table 2. Potentials (mV) for M(III)/M(II) Redox Couples vs $[FeCp_2]^+/FeCp_2$ for Homolpetic and Mixed-Ligand Complexes of Tp and Cp/Cp*[a]

	V		Cr		Fe		Co		Ni	
complex	data	ref	data	ref	data	ref	data	ref	data	ref
MTp_2	−820 (MeCN)[c]	62			−260 (CH_2Cl_2)	this work	−500[e] (CH_2Cl_2)	99	*b*	this work
MTpCp	−760 (CH_2Cl_2) −950 (MeCN)	this work					−590 (CH_2Cl_2)	this work	−420 (CH_2Cl_2)	this work
MTpCp*			−1590[f] (THF)	this work			−890 (CH_2Cl_2)	this work	−385 (CH_2Cl_2)	this work
MTpmCp							−295[g] (CH_2Cl_2)	this work		
MCp_2	−1110 (THF)[c]	100	−960 (MeCN)[d]	32	0		−1350 (CH_2Cl_2)[d]	76	−420 (CH_2Cl_2)[d]	76
MCp^*_2	*a*	32	−1450 (MeCN)[d]	32	−570 (CH_2Cl_2)[c]	76	−1970 (CH_2Cl_2)[d]	76	−1220 (CH_2Cl_2)[d]	76

[a] CV is reported to be complex with no reversible one-electron waves.[32] [b] No redox events observed in solvent window. [c] Value reported vs SCE, corrected to $[FeCp_2]^+/FeCp_2$ using the value quoted for this couple in appropriate solvent/electrolyte combination quoted in ref 101. [d] Values are corrected to $[FeCp_2]^+/FeCp_2$ using the author's own quoted value for this couple in the same solvent/electrolyte combination. [e] Value is measured using Ag/AgCl reference electrode; couple is corrected to SCE using the authors' own correction (E(Ag/AgCl) − E(SCE) = 44 mV in aqueous solution and thence to $[FeCp_2]^+/FeCp_2$ as in footnote *c*. The value is essentially identical to that reported by Trofimenko for the same couple in MeCN (−490 mV, after correction).[86] [f] This couple is quasi-reversible, as indicated by a peak-to-peak separation of 110 mV, which is greater than that of the $[FeCp_2]^+/FeCp_2$ couple (75 mV) under identical conditions. [g] We also observe an irreversible event at −1480 mV in the same solvent attributed to a Co(II)/Co(I) process.

properties and electronic structures of these complexes is in preparation.[45]

Molecular Structures of MCp^RTp Species. Prior to our investigations the structures of RuCpTp and $[RhCp^*Tp]^+[PF_6]^-$ had both been reported and show regular η^5-Cp^R and κ^3-Tp ligation to the metal center.[10,13] We have since communicated the structures of CoCpTp, **6**, and CrCp*Tp, **1**.[25,26] As a consequence of a high-spin d^4 ground state, **1** exhibits Jahn−Teller distortion, resulting in one long and two short Cr−N bonds and considerable variation in the Cr−C bond lengths. **6** displays regular geometry however, but with bond lengths consistent with a high-spin Co(II) center. For η^5-Cp/κ^3-Tp mixed-sandwich complexes two possible ideal conformations can be adopted that preserve maximum symmetry, in this case a mirror plane: these are the "staggered" and "eclipsed" geometries illustrated in Figure 1. RuCpTp and **6** adopt the former, while $[RhCp^*Tp]^+$ adopts the latter conformation. (Three-fold rotational symmetry about the molecular axis requires disorder of the Cp^R ring.) The eclipsed conformation involves direct overlap of a pyrazolyl (pz) group with a ring substituent (either H or Me), whereas a staggered arrangement places two pz rings in close proximity to substituents. We have determined the structures of several of these complexes, and details of the refinements are given in Table 6. Table 7 compares relevant structural parameters for the simple mixed-sandwich species described in this work and also those of **1** and **6**.

Table 3. ^{1}H and $^{11}B\{^{1}H\}$ NMR Spectroscopic Data for 18-Electron Complexes (coupling constants in Hz given in parentheses)

compound	solvent	pzH_3	pzH_4	pzH_5	CpH	Cp*H	Tpm CH	^{11}B
$[CoTp_2]^+[PF_6]^-$ [a]	D_2O	6.67 (2.2)	6.17	8.04 (2.5)				−13.8[e]
$[CoCp^*Tp]^+[PF_6]^-$	$(CD_3)_2CO$	8.82 (2.20)	6.56	7.89 (2.44)		1.55		−6.22[f]
$[CoCpTp]^+[I]^-$	CD_3CN	8.62 (2.20)	6.54	7.85 (2.44)	6.42			−6.12[f]
$[CoCpTpm]^{2+}[PF_6]^-_2$	$(CD_3)_2CO$	9.37 (2.44)	6.94	8.57 (2.93)	7.12		9.33	
$[FeCp^*Tpm]^+[PF_6]^-$	CD_2Cl_2	9.07	6.58	8.12		1.47	8.3	
$[CoCp^*_2]^+[PF_6]^-$ [b]	$(CD_3)_2CO$					1.78		
$[CoCp_2]^+[PF_6]^-$ [c]	$(CD_3)_2CO$				5.95			
$[CoCp^*Cp]^+[PF_6]^-$ [d]	CD_3CN				5.20	2.02		

[a] Data from ref 50. [b] Data from ref 32. [c] Data from ref 102. [d] Data from ref 75. [e] ^{11}B NMR data from ref 103 measured in $(CD_3)_2SO$ and referenced to $B(OMe)_3$ ($\delta = 0$). [f] Referenced to $BF_3{\cdot}Et_2O$.

Table 4. $^{13}C\{^{1}H\}$ NMR Spectroscopic Data for 18-Electron Complexes

compound	solvent	pzC_3	pzC_4	pzC_5	CpC	Cp*Me	Cp* quat	Tpm CH
$[CoTp_2]^+[PF_6]^-$ [a]	D_2O	145.8	110.0	140.0				
$[CoCp^*Tp]^+[PF_6]^-$	$(CD_3)_2CO$	145.8	108.8	138.8		11.4	96.9	
$[CoCpTp]^+[I]^-$	CD_3CN	150.0	109.5	139.9	90.5			
$[CoCpTpm]^{2+}[PF_6]^-_2$	$(CD_3)_2CO$	152.2	110.8	138.3	91.7			74.3
$[FeCp^*Tpm]^+[PF_6]^-$	CD_2Cl_2	147.9	109.2	134.3		10.4	74.4	72.0
$[CoCp^*_2]^+[PF_6]^-$ [b]	$(CD_3)_2CO$					6.3	93.4	
$[CoCp_2]^+[PF_6]^-$ [c]	$(CD_3)_2CO$				85.7			
$[CoCp^*Cp]^+[PF_6]^-$ [d]	CD_3CN				87.5	11.0	98.8	

[a] Data from ref 50. [b] Data from ref 32. [c] Data from ref 102. [d] Data from ref 75.

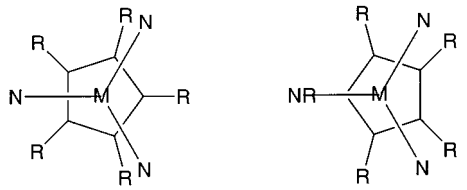

Figure 1. Possible ideal staggered and eclipsed geometries for MCp^RTp complexes (R = Me, H).

A view of the structure of **3** is given in Figure 2. Given that all the other examples of these complexes adopt a κ^3-Tp binding mode, we were somewhat surprised to discover that in this case the Tp ligand is actually κ^2. The molecule sits on a crystallographic mirror plane, which contains the unbound pz ring, B, Co, and C9. The bond lengths around Co are consistent with a low-spin species and much shorter than the corresponding distances in high-spin **6** (see Table 7). The average Co−C bond length (2.078(2) Å) is similar to those observed for a variety of low-spin $Co(II)Cp^R$ complexes,[25] specifically $CoCp_2$ (2.096(8) Å)[46] and CoCp*(acac) (2.089(5) Å).[47] The Co−N bond length (1.931(2) Å) is considerably shorter than that in $CoTp_2$ (2.129(7) Å), which is high-spin also.[48] Although the B−H bond of the Tp ligand points toward the metal center, the Co···H−B distance (3.082 Å) is not indicative of any interaction.

Oxidation of **3** leads to the 18-electron species $\mathbf{3}^+[PF_6]^-$, which adopts a κ^3-Tp structure and a staggered conformation. Two views of the cation are shown in Figure 3. The average Co−N bond length (2.016(2) Å) is somewhat longer than that in crystallographically characterized $[CoTp_2]^+$ cations, 1.918(6)[49] and 1.927(3) Å,[50] and the average Co−C bond length (2.113(3) Å) is longer than observed in comparison to $[CoCp^*_2]^+$ species with a variety of counterions (average Co−C 2.051(6) Å).[51,52] This distance is similar (at the 3σ level) to that in the highly bulky species $[Co(1,2,3,4\text{-}i\text{-}PrCp)_2]^+$ (2.09(1) Å) however.[53] The close proximity of Me groups C15 and C17 to the pz rings containing N3 and N5 results in a compression of the N3−Co−N5 angle as compared to N1−Co−N5 and N1−Co−N3.

By comparison the 18-electron Cp-containing complex $\mathbf{9}^{2+}[PF_6]^-_2$ adopts an eclipsed conformation; two views of the structure of the dication are shown in Figure 4. The average Co−N bond length (1.961(2) Å) is somewhat shorter than that in $\mathbf{3}^+$, as is the average Co−C distance (2.061(2) Å), consistent with a dicationic species. The Co−C bond lengths are longer than those observed in a variety of $[CoCp_2]^+$ salts (Co−C 2.018(5), 2.019(5) Å).[54−56] We are not aware of any other structures of Tpm complexes of Co(III); however the average Co−N bond length is, as expected, substantially shorter than that observed in the Co(II) complex $[Co(Tpm)_2]^{2+}[NO_3]^-_2$ (2.115(3) Å).[57] The structure of the dication is quite regular, as indicated by almost equal N−Co−N and N−C−N angles.

The structure of **4** contains two independent molecules in the asymmetric unit, and a view of one molecule is shown in Figure 5. The structural parameters for both molecules are similar. The Ni−N bond lengths (2.089(3) Å averaged over both molecules) are identical to those in $NiTp_2$ (average 2.093(2) Å).[58] The

(46) Bunder, W.; Weiss, E. *J. Organomet. Chem.* **1975**, *92*, 65−68.
(47) Smith, M. E.; Andersen, R. A. *J. Am. Chem. Soc.* **1996**, *118*, 11119−11128.
(48) Churchill, M. R.; Gold, K.; Maw, C. E. *Inorg. Chem.* **1970**, *9*, 1597−1605.
(49) Curnow, O. J.; Nicholson, B. K. *J. Organomet. Chem.* **1984**, *267*, 257−263.
(50) Hayashi, A.; Nakajima, K.; Nonoyama, M. *Polyhedron* **1997**, *16*, 4087−4095.
(51) Miller, J. S.; Calabrese, J. C.; Harlow, R. L.; Dixon, D. A.; Zhang, J. H.; Reiff, W. M.; Chittipeddi, S.; Selover, M. A.; Epstein, A. J. *J. Am. Chem. Soc.* **1990**, *112*, 5496−5506, and references therein.
(52) Dixon, D. A.; Miller, J. S. *J. Am. Chem. Soc.* **1987**, *109*, 3656−3664.
(53) Burkey, D. J.; Hays, M. L.; Duderstadt, R. E.; Hanusa, T. P. *Organometallics* **1997**, *16*, 1465−1475.
(54) Meng, X.; Waterworth, S.; Sabat, M.; Grimes, R. N. *Inorg. Chem.* **1993**, *32*, 3188−3192.
(55) Jagg, P. N.; Kelly, P. F.; Rzepa, H. S.; Williams, D. J.; Woollins, J. D.; Wylie, W. *J. Chem. Soc., Chem. Commun.* **1991**, 942−944.
(56) Silvestru, A.; Breunig, H. J.; Ebert, K. H.; Kaller, R. *J. Organomet. Chem.* **1995**, *501*, 117−121.
(57) Astley, T.; Gulbis, J. M.; Hitchman, M. A.; Tiekink, E. R. *J. Chem. Soc., Dalton Trans.* **1993**, 509−515.

Table 5. ^{1}H NMR Spectroscopic Data for Paramagnetic Compounds

compound	δ (ppm)	solvent
CrCp*Tp, **1**	85 (Cp*H), 16 (pz$H$), −12 (pz$H$), −50 (pz$H$)	C_6D_6
[CrCp*Tp]$^+$[PF_6]$^-$, **1**$^+$	95, −4, −20	$(CD_3)_2CO$
FeCp*Tp, **2**	47.3 (Cp*H), 23.1 (pz$H$), 15.3 (pz$H$), −6.8 (pz$H$)	C_6D_6
CoCp*Tp, **3**	15, −30	C_6D_6
NiCp*Tp, **4**	45 (pz$H$), 41(pz$H$), 39 (pz$H$), −15 (BH), −90 (Cp*H)	C_6D_6
[NiCp*Tp]$^+$[PF_6]$^-$, **4**$^+$	54 (Cp*H), 28 (pz$H$), 23 (pz$H$), 22 (pz$H$), −5 (BH)	$(CD_3)_2CO$
VCpTp, **5**	11, 9.5, −31, −90	C_6D_6
[VCpTp]$^+$[BAr′$_4$]$^-$, **5**$^+$	12.5, 7.72 (s, 8H, *o*-CH−BAr′$_4$), 7.55 (s, 4H, *p*-CH−BAr′$_4$), 4.5, −29.6	CD_2Cl_2
[VCpTp(MeCN)]$^+$[PF_6]$^-$, **5**(MeCN)$^+$	−1.4	CD_3CN
[VCpTp(CN^{t}Bu)]$^+$[PF_6]$^-$, **5**(CN^{t}Bu)$^+$	7.64 (s, 8H, *o*-CH−BAr′$_4$), 7.48 (s, 4H, *p*-CH−BAr′$_4$), 2.1, −1.9	CD_2Cl_2
[VCpTp(PMe$_3$)]$^+$[PF_6]$^-$, **5**(PMe$_3$)$^+$	7.73 (s, 8H, *o*-CH−BAr′$_4$), 7.56 (s, 4H, *p*-CH−BAr′$_4$), 2.2, −1.9	CD_2Cl_2
CoCpTp, **6**	96.2 (CpH), 65.0 (pz$H$), 50.5 (pz$H$), −64.0 (pz$H$)	C_6D_6
NiCpTp, **7**	52 (pz$H$), 49 (pz$H$), 40 (pz$H$), −10 (BH), −32 (CpH)	C_6D_6
[CoCpTpm]$^+$[PF_6]$^-$, **9**$^+$	94.0 (CpH), 84 (pz$H$), 48.5 (pz$H$), 47 (Tpm CH), −60 (pz$H$)	CD_2Cl_2

Table 6. Details of Crystal Structure Parameters and Refinements

	3	**3**$^+$[PF_6]$^-$	**4**	**5**$^+$[BAr′$_4$]$^-$·2CH_2Cl_2	**5**(MeCN)$^+$[PF_6]$^-$	**5**(PMe$_3$)$^+$[BAr′$_4$]$^-$	**9**$^{2+}$[PF_6]$^-_2$
formula	$C_{19}H_{25}BCoN_6$	$C_{19}H_{25}BCoF_6N_6P$	$C_{19}H_{25}BN_6Ni$	$C_{48}H_{31}B_2C_{14}F_{24}N_6V$	$C_{16}H_{18}BF_6N_7PV$	$C_{49}H_{36}B_2F_{24}N_6PV$	$C_{15}H_{15}CoF_{12}N_6P_2$
fw	407.19	552.16	406.97	1326.15	515.09	1268.37	628.20
size, mm	0.3, 0.2, 0.03	0.16, 0.20, 0.30	0.4, 0.6, 0.6	0.5, 0.3, 0.2	0.3, 0.3, 0.05	0.4, 0.2, 0.2	0.4, 0.4, 0.15
class	ortho	mono	ortho	triclinic	ortho	mono	triclinic
space gp	*Pnma* (62)	*P*2$_1$/*c* (14)	*Pca*2$_1$ (29)	*P*$\bar{1}$ (2)	*Pbca* (61)	*P*2/*c* (13)	*P*$\bar{1}$ (2)
a, Å	11.0641(4)	11.7592(2)	14.356(1)	12.5841(2)	12.000(1)	26.3352(5)	9.9120(1)
b, Å	11.1712(3)	14.5587(3)	19.730(1)	13.7584(2)	15.632(1)	12.7266(2)	10.8257(1)
c, Å	16.1568(7)	13.0853(2)	13.955(1)	17.3823(3)	22.465(1)	16.2206(2)	12.0264(2)
α, deg	90	90	90	110.282(1)	90	90	107.630(1)
β, deg	90	93.16(5)	90	98.276(1)	90	74.064(1)	101.360(1)
γ, deg	90	90	90	99.804(1)	90	90	111.794(1)
V, Å^3	1996.97(12)	2236.8	3952.7	2713.80(7)	4214.1	5227.53(1)	1069.88(2)
Z	4	4	8	2	8	4	2
ρ_{calc}, Mg m^{-3}	1.35	1.64	1.37	1.67	1.62	1.61	1.95
μ, mm^{-1}	0.88	0.91	1.00	0.505	0.619	0.349	1.074
F(000)	852	1132	1720	1356	2080	2544	624
θ range, deg	5.19−27.45	0−27.5	0−26.4	2.46−27.52	5.14−27.48	5.10−27.49	2.22−27.49
total no. of data	4340	22 874	28 467	22 346	8949	18 545	8551
no. of unique data	2385 [*R*(int)=0.0347]	5337 [*R*(int)=0.038]	7623 [*R*(int)=0.043]	12376 [*R*(int)=0.0285]	4796 [*R*(int)=0.0443]	11267 [*R*(int) = 0.0321]	4762 [*R*(int)=0.0114]
no. obs reflns	1808[a]	3708[b]	7156[b]	8954[a]	3278[a]	7896[a]	4530[a]
GOF	1.024	1.041	1.0479	1.028	1.013	1.031	1.230
R indices	R1=0.0363 wR2=0.0759	R1=0.0473 wR2=0.0569	R1=0.0459 wR2=0.0397	R1=0.0644 wR2=0.1674	R1=0.0383 wR2=0.0808	R1=0.0617 wR2=0.1435	R1=0.0383 wR2=0.1051
residuals, e Å^{-3}	0.33, −0.33	−0.68, 1.08	−0.91, 1.18	1.46, −0.89	0.36, −0.33	0.99, −0.54	0.98, −0.61

[a] $I > 2\sigma(I)$. [b] $I > 3\sigma(I)$.

Table 7. Selected Bond Lengths and Angles for Binary MTp(m)Cp^R Complexes

							4	
	5$^+$[BAr′$_4$]$^-$	**1**	**3**	**3**$^+$[PF_6]$^-$	**6**	**9**$^{2+}$[PF_6]$^-_2$	molecule 1	molecule 2
				Bond Lengths (Å)				
M−N	2.059(3)	2.092(2)	1.931(2)	2.009(2)	2.069(2)	1.964(2)	2.053(3)	2.083(3)
	2.055(3)	2.123(2)	1.931(2)	2.006(2)	2.103(1)	1.962(3)	2.085(3)	2.077(3)
	2.024(3)	2.439(2)		2.034(2)	2.103(1)	1.957(2)	2.119(3)	2.116(3)
M−C	2.292(4)	2.372(3)	2.067(2)	2.134(3)	2.268(3)	2.068(2)	2.262(3)	2.238(3)
	2.265(3)	2.296(3)	2.067(2)	2.079(3)	2.286(2)	2.069(2)	2.285(3)	2.278(3)
	2.247(3)	2.319(3)	2.079(2)	2.087(3)	2.286(2)	2.054(2)	2.269(4)	2.288(3)
	2.258(4)	2.317(3)	2.079(2)	2.137(3)	2.305(2)	2.064(2)	2.203(4)	2.266(3)
	2.287(4)	2.399(3)	2.096(3)	2.129(3)	2.305(2)	2.050(2)	2.215(3)	2.237(3)
M−Ct[a]	1.933	2.008	1.686	1.724	1.957	1.672	1.903	1.912
B−N	1.534(5)	1.544(4)	1.551(2)	1.569(4)	1.541(2)	1.453(3)[b]	1.538(5)	1.550(4)
	1.557(4)	1.540(4)	1.551(2)	1.497(4)	1.541(2)	1.444(3)[b]	1.543(5)	1.532(5)
	1.549(4)	1.537(4)	1.518(4)	1.531(4)	1.543(3)	1.446(3)[b]	1.544(5)	1.536(4)
				Bond Angles (deg)				
B−M−Ct[a]	172.4	167.4	146.2	178.2	177.4	178.7[b]	177.3	176.9
N−B−N	107.8(3)	109.0(2)	110.37(16)	108.2(2)	109.26(13)	109.36(17)[b]	109.2(3)	108.5(3)
	108.7(3)	110.0(2)	110.37(16)	108.9(3)	109.26(13)	109.18(17)[b]	108.1(3)	107.2(3)
	106.9(2)	109.1(2)	106.8(2)	105.3(3)	107.04(19)	109.39(18)[b]	106.8(3)	107.8(3)
N−M−N	88.46(10)	88.72(9)	91.82(9)	89.9(1)	88.22(5)	87.30(8)	88.41(11)	88.07(11)
	89.15(11)	82.17(8)		91.46(11)	88.22(5)	89.47(8)	87.66(11)	85.6(1)
	90.35(10)	83.06(8)		83.75(11)	86.00(7)	87.67(8)	85.3(1)	88.3(1)

[a] Ct = Cp(centroid). [b] For these parameters replace B with Tpm apical C (C15).

Ni−C bond lengths (2.254(3) Å) are significantly lengthened compared to the sterically uncrowded systems $NiCp_2$ (average 2.164(7) Å)[59] and bis(isodicyclopentadienyl)Ni(II) (average 2.196(8) Å),[60] but similar to the sterically bulky complex Ni($C_5Ph_4H)_2$ (average 2.22(1) Å).[61] Both molecules are in the staggered conformation,

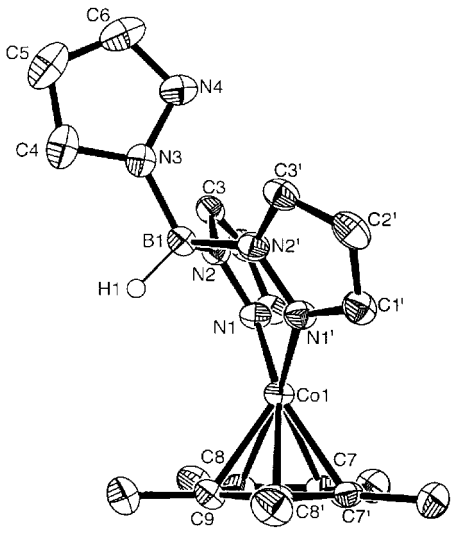

Figure 2. View of structure of **3**, with all H atoms omitted for clarity (except B−H). Thermal ellipsoids are at 50% probability, and primed atoms are generated by symmetry.

and again (as in $\mathbf{3}^+$) there is some closure of the angle between the pz rings in close proximity to the Cp*Me groups.

The structure of $\mathbf{5}^+[BAr'_4]$ confirms that it is a 14-electron sandwich complex with η^5-Cp and κ^3-Tp bonding and no additional ligands. A view of the structure of the cation is given in Figure 6. The cation is in an eclipsed conformation: the average V−N bond length is 2.046(3) Å, which is slightly shorter than the average in $[VTp_2]^+$, 2.073(2) Å.[62] The average V−C bond length is 2.270(4) Å, which is identical to that in $[VCp_2(acetone)]^+$ (2.265(4) Å).[63] The V−Ct (Ct = Cp centroid) distance is shorter than those observed for the only two crystallographically characterized 14-electron planar metallocene species, $Ti(C_5Me_4(SiMe_2Bu^t)_2$ (2.018(4) Å)[64] and $Ti(C_5Me_4(SiMe_3))_2$ (2.020(2) Å).[65] In comparison to the B−V−Ct angles in $\mathbf{3}^+$, $\mathbf{9}^{2+}$, **4**, and **6**, this parameter in $\mathbf{5}^+$ is distinctly nonlinear at 172.4°. The Ct−V−N angle to N3 (132.7°) is opened considerably compared to those to N1 and N5 (121.2° and 122.9°), which is reflected in an inclination of the plane containing the three ligating N atoms of the Tp ligand to the least-squares plane of the Cp ring of 5.3(2)°. This distortion is hard to justify on steric grounds, i.e., due to repulsions between the C3−H bond and the pz ring that eclipses it. $\mathbf{9}^{2+}$ adopts a much more regular geometry but has much shorter M−C and M−N distances (in this instance the angle between the two planes is 0.8° and the Ct−Co−C angle, 178.7°).

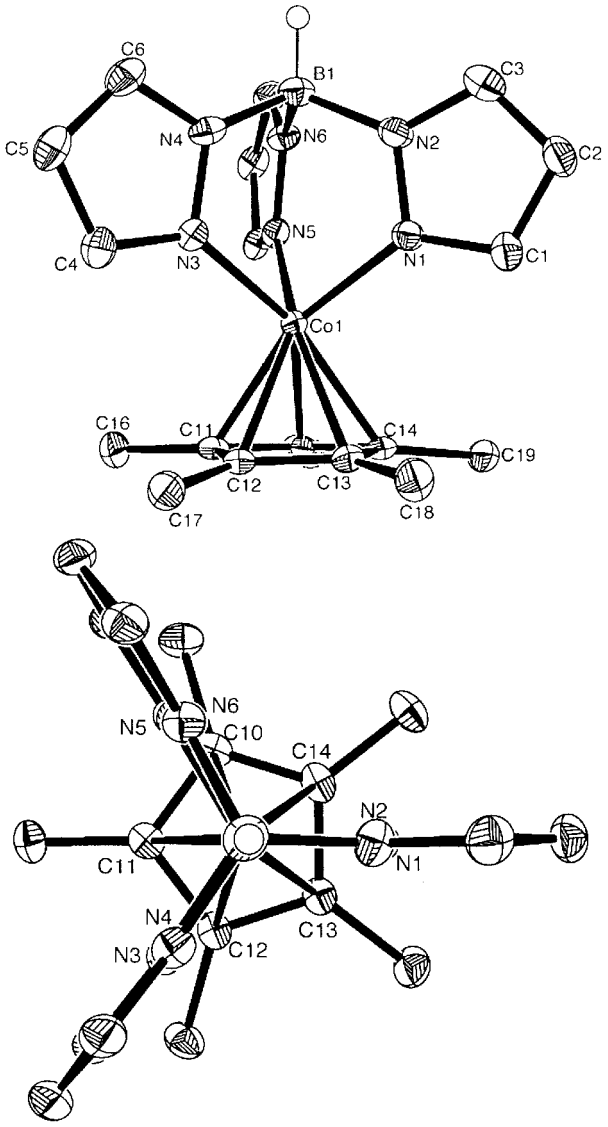

Figure 3. Two views of the structure of $\mathbf{3}^+$ (anion not shown) illustrating the staggered geometry. All H atoms are omitted for clarity (except B−H), and thermal ellipsoids are at 50% probability.

Molecular Structures of $[VCpTpL]^+$ Species. We have also determined the structures of two adducts of $\mathbf{5}^+$, $\mathbf{5}(MeCN)^+[PF_6]^-$ and $\mathbf{5}(PMe_3)^+[BAr'_4]^-$; important bond lengths and angles are detailed in Table 8. A view of the structure of $\mathbf{5}(MeCN)^+[PF_6]^-$ is given in Figure 7. $\mathbf{5}(MeCN)^+$ contains a nine-coordinate V center with η^5-Cp and κ^3-Tp bonding and a terminal nitrile ligand. The angle between the least-squares plane of the Cp ring and the plane of the three N donor atoms is now opened to 21.7(1)°, reducing the Ct−V1−B1 angle to 161.7°. Similar ring-tilting is observed in $[VCp_2L]^+$ species (where L is a unidentate donor), in which Ct−V−Ct angles are found in the range 153.6−130.9°.[66] The V−pyrazolyl(N) bond lengths vary significantly, with V1−N5 being 0.086(2) Å longer than the average of V1−N1 and V1−N3, which are identical. These two short bond lengths are significantly longer than the average V−N distance in $\mathbf{5}^+$. The V−N(MeCN) bond length

(58) Bandoli, G.; Clemente, D. A.; Paolucci, G.; Doretti, L. *Cryst. Struct. Commun.* **1979**, *8*, 965−970.
(59) Seiler, P.; Dunitz, J. D. *Acta Crystallogr., Sect. B* **1980**, *B36*, 2255−2260.
(60) Scroggins, W. T.; Rettig, M. F.; Wing, R. M. *Inorg. Chem.* **1976**, *15*, 1381−1390.
(61) Castellani, M. P.; Geib, S. J.; Rheingold, A. L.; Trogler, W. C. *Organometallics* **1987**, *6*, 1703−1712.
(62) Mohan, M.; Holmes, S. M.; Butcher, R. J.; Jasinski, J. P.; Carrano, C. J. *Inorg. Chem.* **1992**, *31*, 2029−2034.
(63) Gambarotta, S.; Pasquali, M.; Floriani, C.; Chiesa-Villa, A.; Guastini, C. *Inorg. Chem.* **1981**, *20*, 1−1178.
(64) Hitchcock, P. B.; Kerton, F. M.; Lawless, G. A. *J. Am. Chem. Soc.* **1998**, *120*, 10264−10265.
(65) Horacek, M.; Kupfer, V.; Thewalt, U.; Stepnicka, P.; Polasek, M.; Mach, K. *Organometallics* **1999**, *18*, 3572−3578.
(66) Holloway, C. E.; Melnik, M. *J. Organomet. Chem.* **1986**, *304*, 41−82.

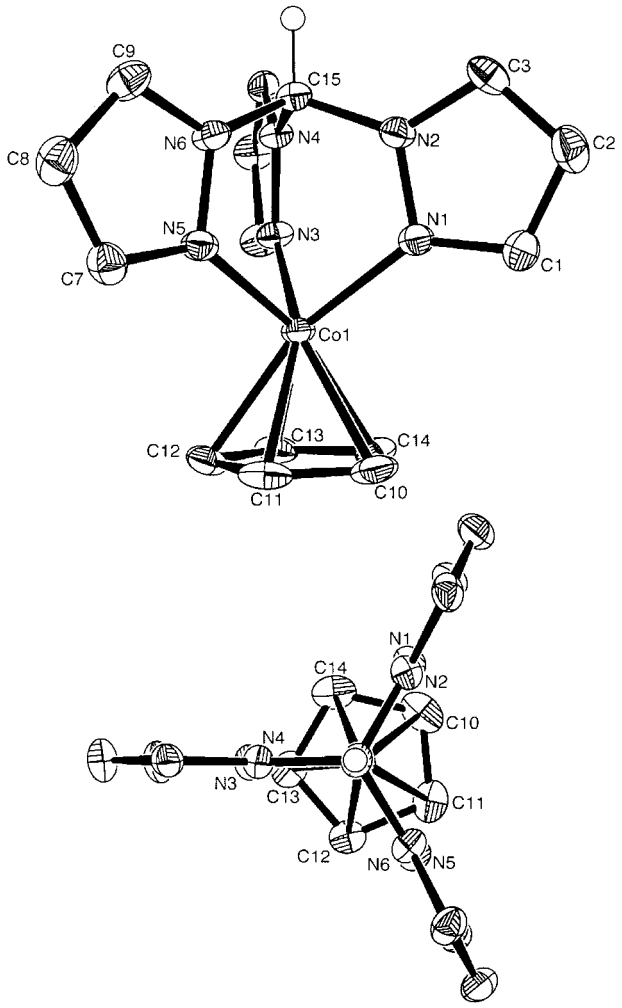

Figure 4. Two views of the structure of $\mathbf{10}^{2+}$ (anions not shown) illustrating the eclipsed geometry. All H atoms are omitted for clarity (except Tpm apical C−H), and thermal ellipsoids are at 50% probability.

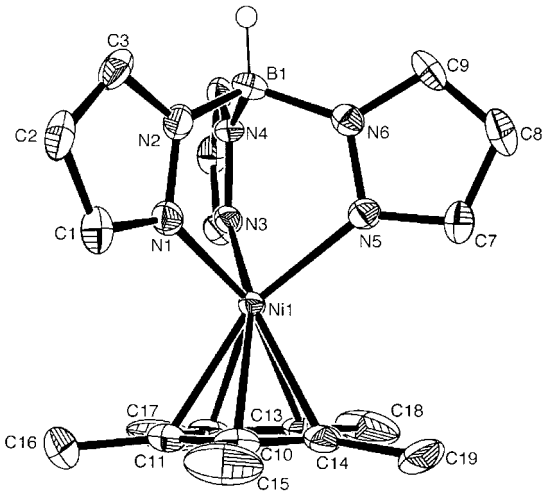

Figure 5. View of structure of **4**, with all H atoms omitted for clarity (except B−H). Thermal ellipsoids are at 50% probability, and only one of the two independent molecules is shown.

(2.165(2) Å) is slightly longer than that observed in other V(III) MeCN complexes: this distance is 2.09(1) Å in $[V_2Fv_2(MeCN)_2]^{2+}$ (Fv = fulvalenyl)[67] and 2.087(4) Å in $[VBr_2(MeCN)_4]^+$.[68] The V−N−C bond angle (to the

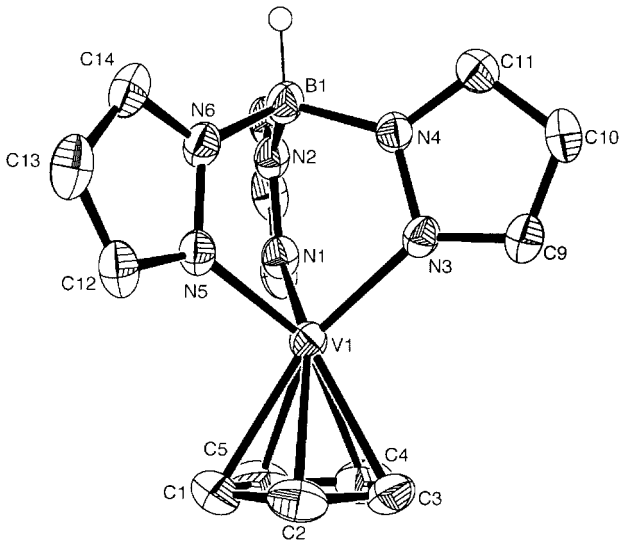

Figure 6. View of the structure of $\mathbf{5}^+$ (anion not shown) with all H atoms omitted for clarity (except B−H). Thermal ellipsoids are at 50% probability.

Table 8. Structural Parameters for $\mathbf{5}(MeCN)^+[PF_6]^-$ and $\mathbf{5}(PMe_3)^+[BAr'_4]^-$

	$\mathbf{5}(MeCN)^+$	$\mathbf{5}(PMe_3)^+$
	Bond Lengths (Å)	
V1−N1	2.094(2)	2.109(2)
V1−N3	2.100(2)	2.105(3)
V1−N5	2.183(2)	2.188(3)
V1−C1	2.271(2)	2.274(3)
V1−C2	2.296(2)	2.318(4)
V1−C3	2.330(2)	2.323(3)
V1−C4	2.333(2)	2.296(3)
V1−C5	2.290(2)	2.258(3)
B1−N2	1.541(3)	1.554(4)
B1−N4	1.534(3)	1.544(4)
B1−N6	1.543(3)	1.546(4)
V1−N7	2.165(2)	
N7−C15	1.139(3)	
V1−P1		2.559(1)
	Bond Angles (deg)	
N1−V1−N3	93.23(7)	95.97(10)
N1−V1−N5	79.69(7)	79.44(9)
N3−V1−N5	81.50(7)	80.09(10)
N1−V1−N7/P1	78.33(7)	78.56(7)
N3−V1−N7/P1	79.74(7)	79.07(7)
N5−V1−N7/P1	150.09(7)	147.75(7)
V1−N7−C15	173.89(17)	
N2−B1−N4	110.84(18)	111.8(3)
N2−B1−N6	105.89(17)	106.1(3)
N6−B1−N4	106.84(18)	105.7(2)
	Torsion Angles (deg)	
V1−N1−N2−C8	167.45	171.46
V1−N3−N4−C11	176.23	178.05
V1−N5−N6−C14	172.13	177.80
V1−N1−N2−B1	16.96	18.50
V1−N3−N4−B1	10.24	14.19
V1−N5−N6−B1	0.54	0.31
	Other Parameters	
V1−Ct[a] (Å)	1.971	1.959
Ct−V1−B1 (deg)	161.69	159.09
ring tilt[b] (deg)	21.66(10)	21.07(18)
Ct−V1−N1 (deg)	133.14	134.09
Ct−V1−N3 (deg)	133.44	129.84
Ct−V1−N5 (deg)	107.16	107.87

[a] Ct = Cp(centroid). [b] Angle between least-squares plane of the Cp ring and plane formed by the three N atoms of the Tp ligand bonded to V.

MeCN ligand) deviates somewhat from linearity, being 173.9(2)°; this may be due to a crystal-packing effect. A view of the cation of $\mathbf{5}(PMe_3)^+[BAr'_4]^-$ is shown in Figure 8. The cation displays a geometry similar to that of $\mathbf{5}(MeCN)^+$, with an almost equal ring tilt and Ct−

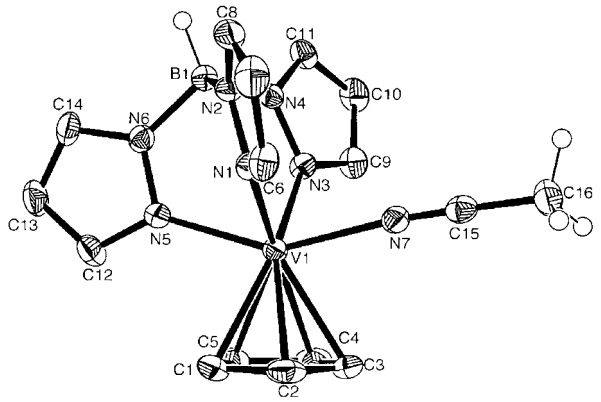

Figure 7. View of the structure of **5**(MeCN)$^+$ (anion not shown) with all H atoms on pyrazolyl and Cp rings omitted for clarity. Thermal ellipsoids are at 50% probability.

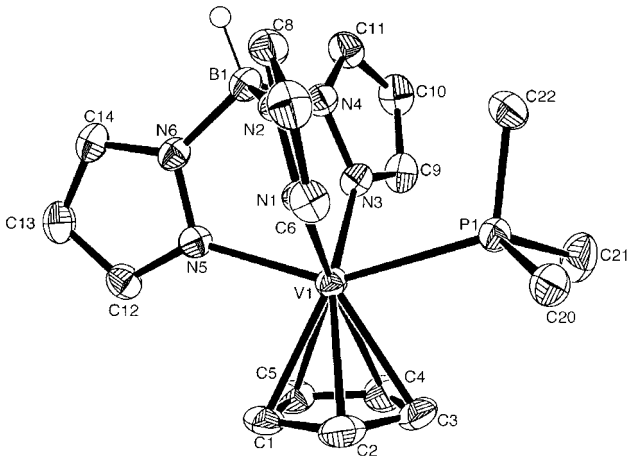

Figure 8. View of the structure of **5**(PMe$_3$)$^+$ (anion not shown) with all H atoms omitted for clarity (except B−H). Thermal ellipsoids are at 50% probability.

V−B angle, and there is no significant difference in the V−N and V−C bond lengths in both cases. The V−P bond (2.559(1) Å) is substantially longer than the average in $[VCp_2(PPhH_2)]^+[BPh_4]^-$ (2.405(4) Å).[69] In an ideal C_{3v} conformation, a TpM fragment should display M−N−N−B torsion angles of 0° and M−N−N−C5 torsion angles of 180°. These angles are listed for **5**(MeCN)$^+$ and **5**(PMe$_3$)$^+$ in Table 8 and indicate that substantial strain in the pz rings adjacent to L is necessary to accommodate this extra ligand.

Discussion

The crystal structures presented above establish the monomeric, axially symmetric nature of the MCpTp class of complexes. The only exception to κ^3-Tp bonding is found in the structure of **3**. Thus replacement of Cp with Cp* in **6**, not only causes a change in the spin state but also causes a dramatic structural change.[25] We will report in more detail on the effect of electronic structure on molecular structure in these systems.[45]

Table 9 summarizes the M−Ct and M−N distances and the conformations adopted by all the crystallographically characterized M*(η^5-Cp^R)(κ^3-Tp/Tpm) complexes. Intraligand repulsions are expected to be greater with Cp* as ligand than with Cp, although it is unclear which conformation should lead to least steric interaction. **3**$^+$ has the shortest M−ligand distances of Cp*-containing complexes and is staggered, whereas [RhCp*Tp]$^+$ with longer M−ligand distances is eclipsed. (The Tp ligand in this complex is significantly twisted out of ideal C_{3v} symmetry to accommodate the intraligand repulsions, and short contact distances between Tp(C) and Cp*(C) atoms between 3.29 and 3.57 Å are observed, which are comparable to those in **3**$^+$). **1** and **4** have staggered conformations, although X-ray data obtained for **4** at room temperature suggest that the Cp* ring is disordered, implying that there is only a small energy difference between both conformations in this structure. Intraligand repulsions may therefore only be significant in affecting the conformation in Cp* complexes with short M−ligand distances. As these parameters lengthen, the exact conformation adopted may depend on crystal-packing forces or electronic effects. For complexes of Cp, there seems to be no real correlation between the conformation adopted and the M−ligand bonding distances. **9**$^{2+}$ shows little distortion in its structure and has the shortest M−Ct and M−N distances of all the complexes studied, yet is eclipsed. **5**$^+$ is also eclipsed with a marked structural distortion, although the M−ligand distances are much longer than those of **9**$^{2+}$. We therefore believe that the distortion in **5**$^+$ has an electronic rather than a steric origin.

Table 9. Conformations and M−Ligand Distances in MCp^{R}Tp Sandwich Complexes

complex	M−Ct (Å)	M−N (av) (Å)	conformation
$[CoCpTpm]^{2+}$, **9**$^{2+}$	1.672	1.961	E
$[CoCp*Tp]^+$, **3**$^+$	1.724	2.016	S
RuCpTp[a]	1.777	2.128	S
$[RhCp*Tp]^+$ [b]	1.820	2.150	E
NiCp*Tp, **4**	1.909[c]	2.089[c]	S
$[VCpTp]^+$, **5**$^+$	1.933	2.046	E
CoCpTp, **6**	1.957	2.092	S
CrCp*Tp, **1**	2.008	2.108[d]	S

[a] Reference 10. [b] Reference 13. [c] Average of both molecules. [d] Average of short Cr−N bond lengths. Ct = Cp(centroid), E = eclipsed, S = staggered.

The value of ν_{B-H} for a Tp′ ligand has recently been used as an indication of its hapticity. Akita et al. found that for κ^2-Tp^{iPr2}ML$_n$ complexes ν_{B-H} was found in the range 2471−2486 cm^{-1}, whereas if bound in a κ^3-mode ν_{B-H} was found in the range 2527−2554 cm^{-1}.[70] Jones et al. have also correlated the ^{11}B NMR shifts of a range of Tp* complexes with its hapticity: κ^3-complexes had resonances between δ −8.44 and −9.76, while κ^2-complexes had resonances between −5.90 and −6.99.[71] From our studies we find that solid-state measurements of ν_{B-H} for crystallographically characterized κ^3-Tp complexes vary between 2460 and 2522 cm^{-1}, whereas the B−H region in the IR spectrum of **3** consists of a strong absorption resolved into three bands, the most intense of which appears at 2435 cm^{-1} (see Table 1). This observation is therefore consistent with Akita's observation that ν_{B-H} for κ^2-Tp complexes is lower in energy than that for κ^3-Tp. We have no structural evi-

(67) Smart, J. C.; Pinsky, B. L.; Fredrich, M. F.; Day, V. W. *J. Am. Chem. Soc.* **1979**, *101*, 4371−4373.
(68) Cotton, F. A.; Lewis, G. E.; Schwotzer, W. *Inorg. Chem.* **1986**, *25*, 3528−3529.
(69) Ho, J.; Breen, T. L.; Ozarowski, A.; Stephan, D. W. *Inorg. Chem.* **1994**, *34*, 865−870.
(70) Akita, M.; Ohta, K.; Takahashi, Y.; Hikichi, S.; Mora-Oka, Y. *Organometallics* **1997**, *16*, 4121−4128.
(71) Northcutt, T. O.; Lachicotte, R. J.; Jones, W. D. *Organometallics* **1998**, *17*, 5148−5152.

dence of the Tp hapticity in $\mathbf{4}^+$ (which is formally isoelectronic with **3**); however ν_{B-H} of 2496 cm^{-1} suggests κ^3-Tp coordination. Several other features are worth noting: first, the range that ν_{B-H} adopts is large, spanning some 62 cm^{-1}, whereas for κ^3-Tp^{iPr2} it was only 27 cm^{-1}. Second ν_{B-H} for the M(III) complex is always higher than for the corresponding M(II) complex; for **6** and $\mathbf{6}^+$ this difference is only 4 cm^{-1}, but for **1** this difference is substantial. Third, for M(II) complexes, those with Cp as ligand all have higher ν_{B-H} than those containing Cp*. These observations suggest some dependence of ν_{B-H} on the oxidation state of a particular metal and on the ancillary ligand, in contradiction to Jones et al.'s observations that δ (^{11}B) and ν_{B-H} are almost solely dependent on hapticity.[71] Interestingly, the ^{11}B chemical shifts observed for $\mathbf{3}^+$ and $\mathbf{6}^+$ (see Table 3) would be indicative of κ^2-coordination from their conclusions.

We were interested to discover whether, in common with other κ^2-Tp′ complexes, **3** is fluxional in solution. Only two broadened ^{1}H NMR resonances are observed in C_6D_6 solution at room temperature, which may be a consequence of the paramagnetism of the Co(II) center, fluxionality, or both. The IR spectrum of **3** in THF solution reveals a ν_{B-H} band at 2462 cm^{-1}, with a shoulder at ~2430 cm^{-1} (the intensity ratio is approximately 2:1). Thus there is an increase in energy of the most intense absorption of 27 cm^{-1} vs the solid-state measurement, suggesting that the κ^3-Tp structure is partially adopted in solution. (This value of ν_{B-H} is almost identical to the solid-state values for other MCp*Tp complexes.) For comparison the IR spectrum of $\mathbf{3}^+$ in CH_2Cl_2 solution has ν_{B-H} at 2504 cm^{-1}, confirming that in this case the solid-state structure remains intact in solution.

In general, the paramagnetic complexes showed relatively well-resolved ^{1}H NMR spectra, and the data are presented in Table 5. In many cases the resonances were assigned by inspection of the relative intensities. Although we have not performed a detailed analysis of the relative contributions of dipolar and contact shifts, it is possible to make comparison between isoelectronic species in cases where we have been unable to obtain susceptibility or structural data. Thus, the spectrum of $\mathbf{9}^+$ is similar to that of isoelectronic **6** and therefore suggests the presence of a high-spin Co(II) center in this case also.[72] A distinctive pattern of three overlapping Tp resonances is observed in a similar chemical shift range for both NiCpTp and NiCp*Tp, also suggesting similar coordination and spin states of the Ni centers.

NMR spectroscopic data for the diamagnetic species are given in Tables 3 and 4, and a labeling scheme is given in Figure 9. An NOE experiment allowed total assignment of the ^{1}H NMR spectrum of $\mathbf{3}^+$. Selective irradiation of the Cp*H signal caused enhancement to the resonance at 8.82 ppm only, allowing this to be assigned as H_3. ^{1}H−^{13}C correlation experiments (gHSQC) were used to assign the ^{13}C NMR spectra. A general observation in Tp complexes is that $^3J(H_4H_5) > {}^3J(H_3H_4)$, and this assignment has also been confirmed by NOE experiments in several cases.[73,74] For

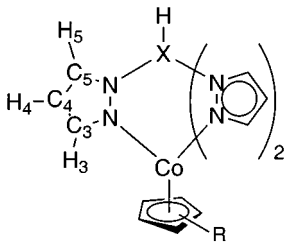

Figure 9. Labeling scheme for NMR assignments of $[CoCp^RTp/Tpm]^{n+}$ species: when X = B, $n = 1$; X = C, $n = 2$. R = H or Me.

$\mathbf{3}^+$ the magnitudes of ^3J were found to be consistent with the previously observed trends with $^3J(H_4H_5) = 2.44$ Hz and $^3J(H_3H_4) = 2.20$ Hz. We were unable to resolve the coupling in the spectrum of $\mathbf{9}^+$; some slight broadening of the resonances is observed, which is probably a consequence of a paramagnetic decomposition product. It is noticeable that H_3 in $[CoTp_2]^+$ is considerably shielded in comparison to the mixed-sandwich species. In the bis(Tp) sandwich complex this proton is situated between two pyrazolyl rings of the second Tp and may experience an aromatic ring shielding current, whereas in our cases these protons point toward the Cp^R ring.[50] The chemical shifts of H_5 are much more similar, as the environment around this proton is not significantly different in these complexes. For the Tp-containing species, the trend in chemical shift $\delta(C_3) > \delta(C_5) > \delta(C_4)$ is the same, supporting the notion that the difference in $\delta(H_3)$ for $[CoTp_2]^+$ is due to a steric influence. Although ^{13}C NMR shifts are subject to many influences, $\delta(C_3)$ and δ(Cp* q) should in some degree reflect the charge density at the metal center, which in turn should be a function of the ancillary ligand. Thus $\delta(C_3)$ for $\mathbf{6}^+$ is significantly deshielded compared to $\delta(C_3)$ for $\mathbf{3}^+$ and $[CoTp_2]^+$, which both occur at a similar shift, suggesting a trend in electron-donating ability, Cp* ≈ Tp > Cp. δ(Cp* q) follows the order $[CoCpCp^*]^+ > \mathbf{3}^+ > [CoCp^*_2]^+$, which suggests a similar ordering in relative electron-donating ability of the three ligands, Cp* > Tp > Cp. Due to the complexity of the factors involved, these trends are at best tentative. As expected, δ(Cp* q) for $\mathbf{9}^+$ is much more shielded than for the Co complexes, reflecting the trend previously observed in 18-electron MCp^*_2 species.[32]

A comparison of electrochemical data for the homoleptic and mixed-sandwich complexes is provided in Table 2. For the metallocenes it is well-established that permethylation of the rings causes a substantial cathodic shift of the M(III)/M(II) couple: for M = Co, this shift is equivalent to about 300 mV per ring,[75] whereas for M = Ni this shift is slightly increased.[76] Both Co(II) compounds **3** and **6** are much less easily oxidized than $CoCp_2$, suggesting that Tp is a worse electron donor than Cp. This is in contrast to the ^{13}C NMR data mentioned above; however we note that the NMR data refer solely to the Co(III) oxidation state, whereas electrochemical data reflect the relative stability of two

(72) An EPR spectrum of this species at 100 K is consistent with a species with a single unpaired electron however. No spectrum is observed at room temperature; see ref 45.

(73) Bortolin, M.; Bucher, U. E.; Ruegger, H.; Venanzi, L. M.; Albinati, A.; Lianza, F.; Trofimenko, S. *Organometallics* **1992**, *11*, 2514−2521.

(74) Jalon, F. A.; Otero, A.; Rodriguez, A. *J. Chem. Soc., Dalton Trans.* **1995**, 1629−1633.

(75) Barlow, S. *Inorg. Chem.* **2001**, *40*, 7047−7053.

(76) Koelle, U.; Khouzami, F. *Angew. Chem., Int. Ed. Engl.* **1980**, *19*, 640−641.

adjacent oxidation states. We also observe a −300 mV shift between the $\mathbf{6}^+/\mathbf{6}$ and $\mathbf{3}^+/\mathbf{3}$ couples; however drawing an analogy with the $CoCp^*_2$ and $CoCp_2$ couples is probably not warranted. The differences in spin states and structures of the reduced species **3** and **6** introduce additional factors such as differences in exchange and reorganization energies, which complicate the situation considerably. For Ni, this trend is not followed, as, somewhat surprisingly, **7** is slightly harder to oxidize than **4**, although the potentials for both are similar to that of $NiCp_2$. For both Ni species we also observed second redox events occurring at +585 mV (**4**, irreversible) and +440 mV (**7**, quasi-reversible) in CH_2Cl_2, which we attribute to M(IV)/M(III) processes (all couples are quoted vs $[FeCp_2]^+/FeCp_2$). Both $NiCp_2$ and $NiCp^*_2$ display fully reversible $[NiCp^R_2]^{2+}/[NiCp_2]^+$ couples,[32,77] and $[NiCp^*_2]^{2+}$ has been chemically isolated and characterized.[32] In general the metallocenes are more electron-rich, although **1** is easier to oxidize even than $CrCp^*_2$. We can attribute this to the high-spin state of the Cr(II) species and thus the substantial stabilization afforded on generation of a stable Cr(III) center. The stability of all the M(III) species is in accord with the preference of the hard N donor ligand for the higher oxidation state. Fewer data are available for comparison with MTp_2 complexes, although we note that the Co(II)-Cp^RTp complexes are easier to oxidize than $CoTp_2$, but oxidation of **5** (in CH_2Cl_2) is harder than for VTp_2. Thus comparison of the electron-donating ability of Cp, Cp*, and Tp should be confined to a per metal basis, as has previously been demonstrated by comparisons of other relevant data.[5]

A further comment is called for on the electrochemical behavior of **5** in MeCN solution. The cyclic voltammogram of $\mathbf{5}(MeCN)^+$ recorded in MeCN solution revealed a reversible redox process attributable to the V(III)/V(II) couple at the same half-wave potential as was observed in the CV of **5** in the same solvent. The cathodic shift of −190 mV of this wave in MeCN to that observed in CH_2Cl_2 can be explained by the stabilizing effect of MeCN coordination on oxidation. However the similar reversibility of the waves in all three cases implies that MeCN addition/desolvation to the cation is fast on the electrochemical time scale.

The isolation of both $\mathbf{5}^+$ and $\mathbf{5}(MeCN)^+$ as stable complexes highlights the intermediate behavior of **5** as compared to the homoleptic sandwich complexes. VTp_2 is oxidized in MeCN solution, but an MeCN solvent adduct is not formed; only the 14-electron six-coordinate cation is isolated.[62] Oxidation of VCp^*_2 in MeCN solution yields the 16-electron MeCN adduct $[VCp^*_2(MeCN)]^+$, and in other coordinating solvents $[VCp^*_2S]^+$; when the oxidation was performed in THF, the product causes polymerization of the solvent.[32] Attempts to desolvate these cations by heating in vacuo led to their decomposition to intractable materials. Oxidation of VCp_2 in acetone led to the isolation of $[VCp_2(acetone)]^+$, containing an η^1-O-coordinated acetone molecule as shown by a single-crystal X-ray structure.[63] Similar behavior with other donor solvents has been reported,[78] including the isolation of $[VCp_2(THF)]^+$.[79] A recent report has described the isolation of "naked" $[VCp_2]^+$, by oxidation of VCp_2 with $[FeCp_2]^+[BPh_4]^-$ in toluene, although it was described as extremely air-sensitive and characterized by its subsequent reaction with CO or Cl^-.[80] One-electron oxidation in the presence of coordinating anions leads to neutral 16-electron complexes VCp^R_2X, e.g., where X = Cl or Br.[81,82] We assume that the enhanced steric bulk of Tp over Cp or Cp* enables the isolation of both stable 14- and 16-electron species for the mixed species. The cone angles for Tp, Cp, and Cp* have been given as 199°,[4] 150°, and 182°,[3] respectively (alternative values of 110° and 142° have been calculated for Cp and Cp*).[83] We investigated the thermal stability of $\mathbf{5}(MeCN)^+[PF_6]^-$ and found that MeCN was liberated by heating a sample at 60 °C/10^{-2} mbar, as indicated by the characteristic color change from blue to orange. The IR spectrum of the product was consistent with the desolvated cation.

Both $[VCp^*_2]^+$ and $[VCp_2]^+$ react with CO and isocyanides to give 18-electron, diamagnetic cations of formula $[VCp^R_2L_2]^+$.[32,82,84] $[VCp_2]^+$ also forms diamagnetic $[VCp_2L_2]^+$ adducts with $L = PhPH_2$ (whose crystal structure has been determined)[69] and L_2 = dppe (diphenylphosphinoethane);[78] in addition, mixed $[VCp_2(CO)L]^+$ adducts (where $L = PEt_3$, PBu^n_3, and pyridine) were also synthesized and found to be diamagnetic.[78] The failure of $\mathbf{5}^+$ to bind CO can be rationalized by consideration of the IR absorption of the isocyanide ligand in $\mathbf{5}(CN^tBu)^+$, which is to higher freqency (2212 cm^{-1}) than that of free CN^tBu (2136 cm^{-1}). This indicates that there is little M→ligand π-back-bonding character to the M−C bond.[6] Thus $\mathbf{5}^+$ is a poor π-base and is therefore unable to stabilize a M−CO bond, CO being a stronger π-acceptor but a weaker σ-donor than isocyanide. In contrast, both $[VCp_2]^+$ and $[VCp^*_2]^+$ form bis(isocyanide) and bis(CO) adducts; the isocyanide stretching frequencies in these cases are lower than those of the free ligands, indicating the increased π-basicity of the V center in these species.[78,82] $\mathbf{5}(CNBu^t)^+$ is thermally unstable at room temperature, whereas $\mathbf{5}(PMe_3)^+$ loses PMe_3 only on heating to 140 °C/10^{-2} mbar. $\mathbf{5}(PMe_3)^+$ is light-sensitive however, decomposing to a brown oil under normal laboratory lighting over several days. The thermal decomposition of both these adducts again yields orange solids whose IR spectra are the same as that for $\mathbf{5}^+[BAr'_4]^-$. Thus $\mathbf{5}^+$ forms stable adducts with strong σ-donor ligands, although these can be decoordinated thermally.

As mentioned previously, our attempts to synthesize MnCpTp, MnCp*Tp, and CrCpTp have failed thus far. The observation of a tendency to high-spin behavior in mixed Cp^R/Tp complexes, illustrated by **1**, **2**, and **6**, as opposed to the lower-spin configurations adopted by their metallocene counterparts, suggests that these complexes, if isolable, would be high spin also. Presum-

(77) Holloway, J. D. L.; Geiger, W. E. *J. Am. Chem. Soc.* **1979**, *101*, 2038−2044.
(78) Fachinetti, G.; Del Nero, S.; Floriani, C. *J. Chem. Soc., Dalton Trans.* **1976**, 1046−1049.
(79) Choukron, R.; Douziech, B.; Pan, C.; Dahan, F.; Cassoux, P. *Organometallics* **1995**, *14*, 4471−4473.
(80) Calderazzo, F.; Ferri, I.; Pampaloni, G.; Englert, U. *Organometallics* **1999**, *18*, 2452−2458.
(81) De Liefde Meijer, H. J.; Janssen, M. J.; Van der Kerk, G. J. M. *Recl. Trav. Chim. Pays-Bas* **1961**, *80*, 831−845.
(82) Gambarotta, S.; Floriani, C.; Chiesi-Villa, A.; Guastini, C. *Inorg. Chem.* **1984**, *23*, 1739−1747.
(83) Davies, C. E.; Gardiner, I. M.; Green, J. C.; Green, M. L. H.; Grebenik, P. D.; Mtetwa, V. S. B.; Prout, K. *J. Chem. Soc., Dalton Trans.* **1985**, 669−683.
(84) Calderazzo, F.; Bacciarelli, S. *Inorg. Chem.* **1963**, *2*, 721−723.

ably the lability associated with high-spin d^5 (and d^4) centers results in the ligand disproportionation reactions observed. We assume our failure to isolate $[CoTp^*Cp]^+$ is a result of unfavorable steric interactions between the 3-Me groups on the Tp* ligand and the Cp ring in either a reaction intermediate or the product. Such species are stable with 4d metals however, as the successful isolation of RuCpTp* and $[RuCpTp^*]^+$ has been reported.[10] The synthesis of RuCp*Tp* failed presumably due to the increased steric bulk of Cp* over Cp.[10] The smaller radii of first-row transition metals may prevent isolation of mixed Tp*/Cp complexes altogether.

Conclusion

We have synthesized a series of stable mixed-sandwich complexes of Cp^R and Tp with a range of first-row transition metals. Electrochemical, structural, and spectroscopic data indicate that these compounds can be considered as intermediate between metallocene and MTp_2 complexes. As well as having a tendency to high-spin electronic configurations, these complexes show a variety of gross and subtle distortions from ideal geometry in their molecular structures. Thus replacement of a Cp^R ligand in a metallocene for Tp has a considerable impact on the electronic structure and properties of the metal center. We intend to report further studies on the electronic structures and bonding in these complexes in due course.

Experimental Details

Unless stated otherwise, all reactions were performed under an inert atmosphere of N_2 using standard Schlenk techniques or in a Vacuum Atmospheres glovebox. Where necessary, solvents were dried by reflux over the appropriate drying agent: sodium−potassium alloy (pentane), potassium (THF), sodium (toluene), sodium-benzophenone (Et_2O), calcium hydride (MeCN, CH_2Cl_2), and anhydrous calcium sulfate, Drierite (acetone). Solvents for NMR spectroscopy of oxygen- or water-sensitive materials were dried by reflux over the appropriate drying agent, potassium (C_6D_6, $C_6D_5CD_3$, and C_4D_8O) and calcium hydride ($CDCl_3$, CD_2Cl_2, and CD_3CN), and purified by trap-to-trap distillation. $(CD_3)_2CO$ was stored over activated 4 Å molecular sieves under N_2.

NMR spectra were recorded using a Varian Unity Plus 500 MHz spectrometer or a Varian Mercury VX-Works 300 MHz spectrometer. Spectra were referenced via the residual protiosolvent peak, and chemical shifts (δ) are quoted in ppm relative to tetramethylsilane at 0 ppm. Oxygen- or water-sensitive samples were prepared using dried solvents under a N_2 atmosphere in a glovebox and were sealed in tubes fitted with Young's type concentric stopcocks. Fourier transform infrared spectra were recorded using a Perkin-Elmer FT1710 spectrometer as KBr disks or as Nujol mulls or thin films between KBr plates. Analyses were performed by the Analytical Department, Inorganic Chemistry Laboratory, Oxford, and mass spectra by the Mass Spectrometry Service, Department of Chemistry, Oxford. Cyclic voltammograms were recorded using a glassy-carbon working electrode and with platinum wire auxiliary and pseudo-reference electrodes. Measurements were made on deoxygenated solutions ca. 5×10^{-4} M in sample and 0.1 M in $[^nBu_4N]^+[PF_6]^-$ as supporting electrolyte. Solvents (THF, CH_2Cl_2, or MeCN) were freshly distilled before use. Measurements on air-sensitive samples were made under a N_2 atmosphere in a specially constructed cell with a sidearm fitted with a Rotaflo tap, and solutions of the sample and supporting electrolyte were transferred via cannula into the cell. Potentials were referenced to the $[FeCp_2]^+/FeCp_2$ couple at 0 mV by addition of $FeCp_2$ to the cell. The reversibility of the redox couple was judged by comparison with the behavior of the $[FeCp_2]^+/FeCp_2$ couple under the same conditions. Magnetic measurements were performed as described previously.[85] KTp and KTp*,[86] $[CrCp^*Cl]_2$,[87] $[FeCp_2]^+[PF_6]^-$, $[FeCp^*(MeCN)_3]^+[PF_6]^-$,[88] $[CoCp^*Cl]_2$,[89] $NiCp^*(acac)$,[90] VCp_2Cl,[91] $[FeCp_2]^+[BAr'_4]^-$,[38] $CoCp(CO)I_2$,[92] $CoCp_2$,[93] $[NiCp(COD)]^+[BF_4]^-$,[41] and Tpm[94] were prepared by published procedures.

Synthesis of CrCp*Tp, 1. $[CrCp^*Cl]_2$ (0.53 g, 1.19 mmol) was dissolved in THF (20 mL), and a solution of KTp (0.60 g, 2.38 mmol) in THF (10 mL) was added dropwise. The reaction mixture was stirred for 1.5 h at room temperature, and then all volatiles were removed in vacuo. The residues were extracted with pentane (40 mL) to yield a dark green solution. This solution was reduced in volume by ca. 5 mL, whereupon some pale solids precipitated. The solution was filtered to remove this solid and then cooled to −35 °C to yield dark purple crystals of **1**. Crystals suitable for single-crystal X-ray diffraction were grown by slow cooling of a saturated pentane solution to −35 °C. Yield: 0.35 g (0.87 mmol, 36.7%).

Synthesis of $[CrCp^*Tp]^+[PF_6]^-$, $1^+[PF_6]^-$. CrCp*Tp (0.20 g, 0.50 mmol) was dissolved in THF (10 mL), and a suspension of $[FeCp_2]^+[PF_6]^-$ (0.16 g, 0.48 mmol) in THF (15 mL) was added dropwise. During the addition a dark solid was seen to precipitate, and the solution turned light brown. The reaction mixture was stirred for 1 h and allowed to settle, and the resultant purple precipitate was isolated by filtration. It was then washed with Et_2O (2 × 5 mL) and dried in vacuo. The solids were redissolved in the minimum volume of MeCN (20 mL), stirred, and reprecipitated by the dropwise addition of Et_2O (100 mL) to this solution. The precipitate was dried in vacuo to yield analytically pure solid. Yield: 0.19 g (0.35 mmol, 73.3% based on $[FeCp_2]^+$).

Synthesis of FeCp*Tp, 2. $[FeCp^*(MeCN)_3]^+[PF_6]^-$ (0.43 g, 0.93 mmol) was dissolved, and MeCN (15 mL) and a solution of KTp (0.23 g, 0.93 mmol) in MeCN (10 mL) were added dropwise with stirring. The reaction mixture turned dark green by the end of the addition and was stirred for a further 40 min. All volatiles were then removed in vacuo, and the residue was extracted with pentane (total 30 mL). The blue-green solution was reduced slightly in volume and cooled to −30 °C for 12 h to yield a mixture of **2** as fine blue-green needles and $FeTp_2$ as pale pink blocks. Analytically pure samples were obtained by manual separation of the crystals: pure solutions of **2** were obtained by addition of the minimum volume of precooled (−40 °C) acetone necessary to dissolve **2** and filtration while maintaining this temperature. Total yield of **2** and $FeTp_2$: 0.10 g.

Synthesis of CoCp*Tp, 3. $[CoCp^*Cl]_2$ (0.20 g, 0.44 mmol) was dissolved in THF (10 mL), and a solution of KTp (0.21 g, 0.87 mmol) in THF (10 mL) was added dropwise with stirring. Over the course of the addition the deep brown solution lightened to a red-orange color. The reaction mixture was stirred for 1 h, and then all volatiles were removed in vacuo and the sticky residue was dried thoroughly. The resultant red solid was extracted with pentane (3 × 15 mL), and the solution was reduced in volume by ∼5 mL. A small amount of

(85) Brunker, T. J.; Hascall, T.; Cowley, A. R.; Rees, L. H.; O'Hare, D. *Inorg. Chem.* **2001**, *40*, 3170−3176.
(86) Trofimenko, S. *J. Am. Chem. Soc.* **1967**, *89*, 3170−3177.
(87) Heinitz, R. A.; Ostrander, R. L.; Rheingold, A. L.; Theopold, K. H. *J. Am. Chem. Soc.* **1994**, *116*, 11387−11396.
(88) Catheline, D.; Astruc, D. *Organometallics* **1984**, *3*, 1094−1100.
(89) Koelle, U.; Fuss, B.; Belting, M.; Raabe, E. *Organometallics* **1986**, *5*, 980−987.
(90) Bunel, E. E.; Valle, L.; Manriquez, J. M. *Organometallics* **1985**, *4*, 1680−1682.
(91) Manzer, L. E. *Inorg. Synth.* **1990**, *28*, 260−263.
(92) King, R. B. *Inorg. Chem.* **1966**, *5*, 82−87.
(93) Wilkinson, G.; Cotton, F. A.; Birmingham, J. M. *J. Inorg. Nucl. Chem.* **1956**, *2*, 95−113.
(94) Reger, D. L.; Grattan, T. C.; Brown, K. J.; Little, C. A.; Lamba, J. J. S.; Rheingold, A. L.; Sommer, R. D. *J. Organomet. Chem.* **2000**, *607*, 120−128.

yellow solid precipitated which did not redissolve on warming, so the solution was refiltered and cooled to −30 °C for 24 h to yield **3** as a red-brown crystalline solid. Further concentration and cooling of the supernatant to −30 °C yielded a further crop of solid. Single crystals suitable for X-ray diffraction were grown by slow-cooling a pentane solution to −30 °C. Yield: 0.15 g (0.37 mmol, 42.3%).

Synthesis of [CoCp*Tp]$^+$[PF$_6$]$^-$, 3$^+$[PF$_6$]$^-$. 3 (0.13 g, 0.32 mmol) was dissolved in dry MeCN (20 mL) to give a red-brown solution, and a solution of [FeCp$_2$]$^+$[PF$_6$]$^-$ (0.10 g, 0.30 mmol) in MeCN (7 mL) was added dropwise with stirring. Upon addition the solution darkened instantly, and on completion was dark blue-purple in color. The reaction was stirred for 1 h, and then all volatiles were removed in vacuo to yield a deep purple solid. This was washed with Et$_2$O (5 × 5 mL) to remove FeCp$_2$ and unreacted **3**, and the residue was dried in vacuo. Redissolution of this solid in dry acetone (20 mL) and precipitation with pentane (∼50 mL) gave analytically pure **3**$^+$[PF$_6$]$^-$ as an air-stable blue-purple powder. Single crystals were grown by slow evaporation of a CH_2Cl_2 solution. Yield: 0.12 g (0.21 mmol, 70.2% based on [FeCp$_2$]$^+$).

Synthesis of NiCp*Tp, 4. NiCp*(acac) (0.30 g, 1.04 mmol) was dissolved in THF (15 mL), and a solution of KTp (0.26 g, 1.04 mmol) in THF (15 mL) was added dropwise. During the addition a white solid was seen to precipitate and an orange-brown solution formed. The reaction mixture was stirred for 1 h and then stripped to dryness in vacuo. The residues were extracted with pentane (3 × 20 mL) to give a golden-brown solution. Concentration of this solution by ca. 15 mL and cooling to −35 °C for 12 h yielded golden-brown microcrystals of **4**. Further concentration and cooling yielded further crops of solid. Single crystals suitable for X-ray diffraction were grown by slow cooling of a concentrated pentane solution to −35 °C. Yield: 0.30 g from 3 crops (0.74 mmol, 70.8%).

Synthesis of [NiCp*Tp]$^+$[PF$_6$]$^-$, 4$^+$[PF$_6$]$^-$. [FeCp$_2$]$^+$[PF$_6$]$^-$ (0.19 g, 0.58 mmol) was stirred as a suspension in CH_2Cl_2 (15 mL), and a solution of **4** (0.25 g, 0.61 mmol) in CH_2Cl_2 (10 mL) was added dropwise. Over the course of the addition a dark solution formed, from which a dark solid precipitated on continued stirring. The reaction mixture was stirred for a further hour and the precipitate isolated by filtration as a black powder. This was washed with Et$_2$O (2 × 10 mL) and dried in vacuo to give analytically pure **4**$^+$[PF$_6$]$^-$. Further product could be isolated from the CH_2Cl_2 supernatant by addition of Et$_2$O (100 mL) dropwise with stirring. The resultant black-brown solid was isolated by filtration and dried in vacuo. Elemental analysis of this material was close to that calculated for **4**$^+$[PF$_6$]$^-$, and its IR spectrum was similar to that of the first sample. Yield: 0.19 g combined yield (0.34 mmol, 56.1%).

Synthesis of VCpTp, 5. This preparation is a modification of a literature procedure.[14] VCp$_2$Cl (1.50 g, 6.93 mmol) was dissolved in THF (25 mL), and a solution of KTp (1.73 g, 6.93 mmol) in THF (20 mL) was added dropwise. During the addition the dark blue solution gradually turned dark green. The reaction mixture was stirred at room temperature for 2 h, and then all volatiles were removed and the residue was thoroughly dried in vacuo. The green-purple solid residue was extracted with Et$_2$O (2 × 25 mL) to give a dark solution. The solution was reduced in volume by 15 mL and cooled to −35 °C for 24 h to yield a dark green crystalline solid. This solid was washed with precooled Et$_2$O (5 mL) at −80 °C to remove a purple oily contaminant and dried in vacuo to give analytically pure **5**. Yield (in 3 crops): 1.30 g (4.00 mmol, 56.8%).

Synthesis of [VCpTp(MeCN)]$^+$[PF$_6$]$^-$, 5(MeCN)$^+$[PF$_6$]$^-$. A solution of [FeCp$_2$]$^+$[PF$_6$]$^-$ (0.20 g, 0.60 mmol) in MeCN (10 mL) was added dropwise to a solution of **5** (0.20 g, 0.61 mmol) in MeCN (15 mL), yielding a dark green solution. The reaction mixture was stirred for 1 h, and then all volatiles were removed in vacuo. The residues were washed with pentane (5 × 10 mL), and the resultant blue-green solid was dried in vacuo. The solid was redissolved in MeCN (10 mL) and filtered and toluene (30 mL) added, yielding a blue-green microcrystalline precipitate, which was isolated by filtration, washed with pentane (5 mL), and dried in vacuo. Further addition of toluene to the supernatant and cooling to −30 °C produced a second crop of solid. Single crystals suitable for X-ray diffraction were grown by layering a concentrated MeCN solution with Et$_2$O. Yield: 0.20 g (0.39 mmol, 64.9% based on ferrocenium).

Synthesis of [VCpTp]$^+$[BAr′$_4$]$^-$, 5$^+$[BAr′$_4$]$^-$. 5 (0.15 g, 0.46 mmol) and [FeCp$_2$]$^+$[BAr′$_4$]$^-$ (0.50 g, 0.46 mmol) were placed in a Schlenk vessel under N$_2$, and CH_2Cl_2 (15 mL) was added with stirring. All the solids instantly dissolved, forming a dark red solution. The reaction mixture was stirred for 15 min, and then all volatiles were removed in vacuo. The residues were washed with pentane (4 × 10 mL) to remove FeCp$_2$, and the red-brown residue was dried in vacuo. The solids were then redissolved in CH_2Cl_2 (10 mL), and the solution was filtered into an ampule and layered with pentane (50 mL). Dark red crystals suitable for single-crystal X-ray diffraction were isolated after 24 h; these were found to be of composition [CpVTp]$^+$[BAr′$_4$]$^-$·2CH_2Cl_2. Crystals dried thoroughly in vacuo analyzed for **5**$^+$[BAr′$_4$]$^-$ with no solvent of crystallization. Yield: 0.43 g (0.36 mmol, 78.2%).

Synthesis of [VCpTp(CN^{t}Bu)]$^+$[BAr′$_4$]$^-$, 5(CN^{t}Bu)$^+$[BAr′$_4$]$^-$. 5 (0.12 g, 0.35 mmol) and [FeCp$_2$]$^+$[BAr′$_4$]$^-$ (0.35 g, 0.33 mmol) were dissolved in CH_2Cl_2 (15 mL) with stirring, forming a red solution. This was stirred for 15 min, and then CNBu^t (0.1 mL) was added by syringe, instantaneously generating a green solution. The reaction mixture was stirred for a further 5 min, and then all volatiles were removed in vacuo. FeCp$_2$ was removed by washing with pentane (4 × 10 mL), to yield a blue-green powder, which was dried in vacuo. The solids were redissolved in CH_2Cl_2 (10 mL), the solution was filtered, and the product precipitated by the dropwise addition of pentane (30 mL) while stirring. The blue-green microcrystalline precipitate was isolated by filtration and dried in vacuo. Yield: 0.25 g (0.19 mmol, 55.0% based on [FeCp$_2$]$^+$).

Synthesis of [VCpTp(PMe$_3$)]$^+$[BAr′$_4$]$^-$, 5(PMe$_3$)$^+$[BAr′$_4$]$^-$. 5 (0.10 g, 0.30 mmol) and [FeCp$_2$]$^+$[BAr′$_4$]$^-$ (0.31 g, 0.30 mmol) were dissolved in CH_2Cl_2 (15 mL) with stirring, forming a red solution. This solution was stirred for 15 min and then cooled to −78 °C. The Schlenk was placed under partial vacuum; a small amount of PMe$_3$ was then vacuum transferred into the reaction mixture, causing the solution to immediately assume a dark green coloration. The solution was allowed to warm to room temperature under N$_2$, and then all volatiles were removed in vacuo. FeCp$_2$ was removed by washing with pentane (3 × 15 mL) and the resultant green-blue solid dried in vacuo. This solid was redissolved in CH_2Cl_2 (8 mL) and filtered, and the product was precipitated by dropwise addition of pentane (25 mL). It was isolated by filtration, washed with pentane (5 mL), and dried in vacuo to yield a light gray-blue microcrystalline solid. Single crystals were grown by layering of a concentrated CH_2Cl_2 solution with pentane. Yield: 0.27 g (0.21 mmol, 72.0% based on [FeCp$_2$]$^+$).

Synthesis of [CoCpTp]$^+$[I]$^-$, 6$^+$[I]$^-$. A solution of KTp (0.62 g, 2.46 mmol) in THF (15 mL) was added dropwise to a deep purple solution of CoCp(CO)I$_2$ (1.00 g, 2.46 mmol) in THF (15 mL). The resulting dark suspension was stirred for 15 h, and then the solids were collected on a glass sintered frit. The solids were washed with deionized H_2O (2 × 15 mL), THF (1 × 3 mL), and Et$_2$O (1 × 5 mL) and then dried thoroughly in vacuo. Additional purification was achieved by dissolving the deep purple solids in the minimum volume of $MeNO_2$ (60 mL) and precipitating the product by dropwise addition of Et$_2$O to this solution, with stirring. The product was isolated by filtration as an air-stable purple microcrystalline powder and dried in vacuo. Yield: 1.12 g (2.42 mmol, 98.1%).

Synthesis of [CoCpTp]$^+$[PF$_6$]$^-$, 6$^+$[PF$_6$]$^-$. 6$^+$[I]$^-$ (0.50 g, 1.08 mmol) and $NaPF_6$ (0.20 g, 1.200 mmol) were placed in a thick-walled ampule under N$_2$, and a degassed mixture of H_2O and MeOH (4:1, 50 mL) was added. The ampule was partially

evacuated and heated at 70 °C with stirring for 3 h. The purple insolubles were collected on a glass sintered frit and washed with deionized H_2O (20 mL) and then Et_2O (15 mL). The powder was then dried in vacuo, dissolved in MeCN (30 mL), and filtered, and Et_2O (70 mL) was added dropwise with stirring. The resultant purple powder was isolated by filtration and dried in vacuo. Yield: 0.35 g (0.73 mmol, 67.5%).

Synthesis of CoCpTp, 6. 6$^+$[I]$^-$ (0.28 g, 0.61 mmol) was stirred as a suspension in THF (15 mL), and a solution of $CoCp_2$ (0.11 mg, 0.59 mmol) in THF (8 mL) was added dropwise with stirring. Immediately a yellow precipitate formed, and after the addition was complete the reaction was stirred for a further 30 min, yielding a dark yellow solution and a yellow precipitate of $[CoCp_2]^+[I]^-$. The solution was filtered off and the solids were washed with a further portion of THF (3 mL). The filtrate and washings were combined and stripped to dryness in vacuo. The dirty yellow residue was extracted with pentane (35 mL), concentrated slightly, and cooled to −30 °C overnight to yield yellow-green microcrystals of **6**. Single crystals were grown by slow cooling a saturated pentane solution to −30 °C. Yield: 0.17 g (0.50 mmol, 82.6%).

Synthesis of NiCpTp, 7. [NiCp(1,5-cyclooctadiene)]$^+$[BF_4]$^-$ (0.25 g, 0.78 mmol) was dissolved in dry acetone and a solution of KTp (0.20 g, 0.78 mmol) added dropwise. The reaction mixture was stirred for 1 h, during which time a lot of white precipitate formed. All volatiles were then removed in vacuo, and the dirty green residue was extracted with pentane (20 mL). The mid-green solution was reduced slightly in volume and cooled to −35 °C. The first crop isolated contained a few pale green needles of **7** and some pink crystalline material identified as $NiTp_2$ by EA and IR. Further concentration and cooling yielded further quantities of **7**, although these crops were found to be contaminated with $NiCp_2$ also. **7** can be separated from $NiCp_2$ by sublimation of the metallocene at 50 °C/10^{-2} mbar onto a coldfinger. It must be noted that on each occasion this reaction was performed, differing amounts of each product were formed despite attempting to reproduce the same conditions as previously.

Synthesis of [FeCp*Tpm]$^+$[PF_6]$^-$, 8$^+$[PF_6]$^-$. [FeCp*(MeCN)$_3$]$^+$[PF_6]$^-$ (0.50 g, 1.16 mmol) was dissolved in MeCN (10 mL), and a solution of Tpm (0.25 g, 1.16 mmol) in MeCN (10 mL) was added dropwise with stirring. Over the addition the dark purple solution turned dirty green in color. The reaction mixture was then stirred for a further 15 min, and then the volume of the solution reduced by about one-third. Et_2O (100 mL) was added dropwise with stirring to precipitate a dark green powder. This was isolated by filtration, washed with Et_2O (10 mL), and dried in vacuo. Yield: 0.31 g (0.78 mmol, 67%).

Synthesis of [CoCpTpm]$^{2+}$[I]$^-_2$, 9^{2+}[I]$^-_2$. $CoCp(CO)I_2$ (2.00 g, 4.93 mmol) and Tpm (1.06 g, 4.93 mmol) were placed in a Schlenk vessel, and THF (40 mL) was added. The reaction mixture was stirred for 1.5 h at ambient temperature, and the resultant dark precipitate was then collected on a glass-sintered frit. The solids were washed with Et_2O (∼30 mL) until the washings were colorless, and the dark purple solid was dried in vacuo. The product was shown to be essentially pure by ^{1}H NMR spectroscopy (D_2O): further purification was achieved by metathesis to the PF_6^- salt. Yield: 2.74 g (4.63 mmol, 93.9%).

Synthesis of [CoCpTpm]$^{2+}$[PF_6]$^-_2$, 9^{2+}[PF_6]$^-_2$. 9^{2+}[I]$^-_2$ (1.20 g, 2.03 mmol) was dissolved in H_2O (170 mL), and the solution degassed with N_2 and then added dropwise to a stirred, degassed solution of $NaPF_6$ (1.00 g, 5.95 mmol) in H_2O (10 mL). During the addition a purple precipitate formed, which was then allowed to settle. The supernatnant was decanted, and the solids were washed with H_2O (15 mL) and then dried thoroughly in vacuo. The residue was redissolved in acetone (20 mL) and filtered. This solution was vigorously stirred, and the product was precipitated by dropwise addition of pentane (∼30 mL). **9**$^{2+}$[PF_6]$^-_2$ was isolated by filtration as a microcrystalline purple solid, washed with pentane (10 mL), and dried in vacuo. Single crystals of **9**$^{2+}$[PF_6]$^-_2$ suitable for X-ray crystallography were gradually deposited from the H_2O supernatant. Yield: 1.07 g (1.70 mmol, 83.9%).

Reduction of 9^{2+}[PF_6]$^-_2$. 9^{2+}[PF_6]$^-_2$ (0.32 g, 0.50 mmol) was stirred as a suspension in THF (20 mL) and a solution of $CoCp_2$ (0.10 g, 0.53 mmol) in THF (10 mL) added dropwise. During the course of the addition the purple solids dissolved and a yellow precipitate formed. The reaction mixture was stirred for a further 20 min and was then filtered. The solids were washed with THF (5 mL), and the washings and filtrate were combined and stripped to dryness in vacuo. The dirty yellow residue was then washed with Et_2O (2 × 10 mL) and the resulting yellow solid dried in vacuo. It was extracted with CH_2Cl_2 (20 mL) and stirred, and pentane (30 mL) was added to precipitate the product as a yellow solid. ^{1}H NMR spectroscopy and elemental analysis revealed this solid to be a mixture of [Cp*CoTpm]$^+$[PF_6]$^-$, **9**$^+$[PF_6]$^-$, and [$CoCp_2$]$^+$.

Crystal Structure Determinations. Crystals were mounted on glass fibers using perfluoropolyether oil, transferred to a goniometer head on the diffractometer, and cooled rapidly to 150(2) K in a stream of cold N_2 using an Oxford Cryostream 600 series. Data collections were performed using an Enraf-Nonius DIP2000 image plate diffractometer (**4**) or an Enraf-Nonius FR590 Kappa CCD (**3**, **3**$^+$[PF_6]$^-$, **5**$^+$[BAr′$_4$]$^-$, **5**(MeCN)$^+$[PF_6]$^-$, **5**(PMe_3)$^+$[BAr′$_4$]$^-$, **8**, **9**$^{2+}$[PF_6]$^-_2$) both utilizing Mo Kα X-ray radiation (λ = 0.71073 Å). The data were processed using the programs DENZO and SCALEPACK.[95] Structures were solved using the direct-methods program SIR-92[96] or SHELXS[97] and refined using full-matrix least-squares refinement on all F data using the CRYSTALS program suite[98] (**4**) or using all F^2 data using SHELX-97 (**3**, **3**$^+$[PF_6]$^-$, **5**$^+$[BAr′$_4$]$^-$, **5**(MeCN)$^+$[PF_6]$^-$, **5**(PMe_3)$^+$[BAr′$_4$]$^-$, **8**, **9**$^{2+}$[PF_6]$^-_2$).[97] In general, all non-hydrogen atoms were refined anisotropically and hydrogen atoms were included in calculated positions with isotropic thermal parameters. **3** crystallized in space group *Pnma* and with half a molecule in the asymmetric unit astride a mirror plane. **5**$^+$[BAr′$_4$]$^-$ crystallized in space group $P\bar{1}$ with a cation, an anion, and two molecules of CH_2Cl_2 in the asymmetric unit. **5**(PMe_3)$^+$[BAr′$_4$]$^-$ crystallized in the monoclinic space group *P*2/*c* with a cation and two-half anions in the asymmetric unit. Each B atom of the two half [BAr′$_4$]$^-$ anions sits on a special position corresponding to a 2-fold rotation axis.

Acknowledgment. We thank Dr. Stephen Barlow for useful discussions, Dr. Tony Hascall for crystallographic assistance, and Simon Jones and Victoria Beck for generous donations of some reagents. We also acknowledge the EPSRC for financial support (T.J.B.).

OM0200149

(95) Otinowski, Z.; Minor, W. *Processing of X-ray Diffraction Data Collected in Oscillation Mode*, *Methods Enzymol.* **1997**, *276*, 307−326; Carter C. W., Sweet, R. M., Eds.; Academic Press: New York.

(96) Altomare, A.; Cascarano, G.; Giacovazzo, G.; Guagliardi, A.; Burla, M. C.; Polidori, G.; Camalli, M. *J. Appl. Crystallogr.* **1994**, *27*, 343−350.

(97) Sheldrick, G. M. *SHELXS*; 1998.

(98) Watkin, D. J.; Prout, C. K.; Carruthers, J. R.; Betteridge, P. W. *CRYSTALS issue 10*; Chemical Crystallography Laboratory: Oxford, UK, 1996.

(99) Janiak, C.; Scharmann, T. G.; Green, J. C.; Parkin, R. P. G.; Kolm, M. J.; Riedel, E.; Mickler, W.; Elguero, J.; Claramunt, R. M.; Sanz, D. *Chem. Eur. J.* **1996**, *2*, 992−1000.

(100) Connelly, N. G.; Davies, J. D. *J. Organomet. Chem.* **1972**, *38*, 385−390.

(101) Connelly, N. G.; Geiger, W. E. *Chem. Rev.* **1996**, *96*, 877−910.

(102) Materikova, R. B.; Babin, V. N.; Lyatifov, I. R.; Salimov, R. M.; Fedin, E. I.; Petrovskii, P. V. *J. Organomet. Chem.* **1981**, 259−267.

(103) Fujihara, T.; Schonherr, T.; Kaizaki, S. *Inorg. Chim. Acta* **1996**, *249*, 135−141.